Synergies between CMB and SKA radio observations

Carlo Burigana
@ INAF/IASF Bologna

thanks to
Planck & PRISM Coll.s
& Italian SKA WG
for related topics

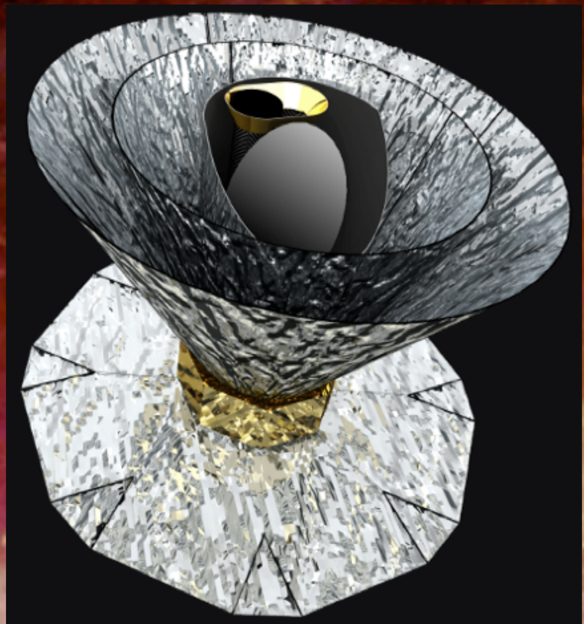

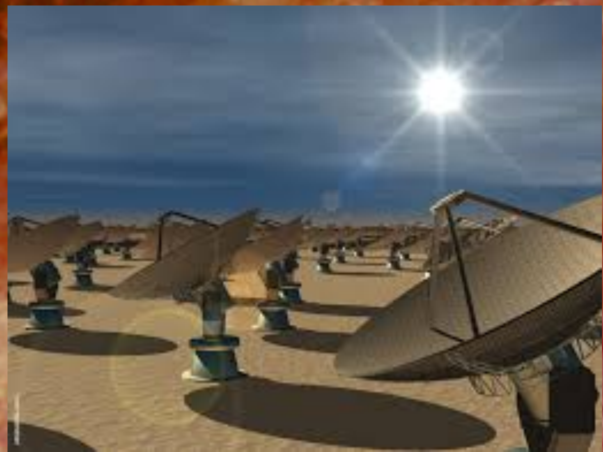

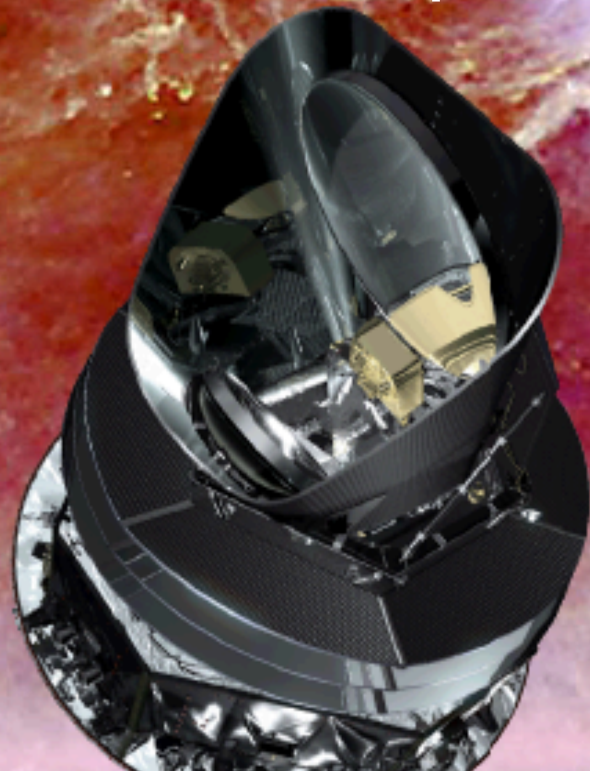

The 18th Paris Cosmology Colloquium Chalonge 2014
"Latest News from the Universe: LambdaWDM, CMB, Warm Dark Matter, Dark Energy, Neutrinos and Sterile Neutrinos",
Observatoire de Paris HQ, Paris campus,
Historic Perrault building, 23-25 July 2014

The CMB seen by *Planck* & its cosmological implications

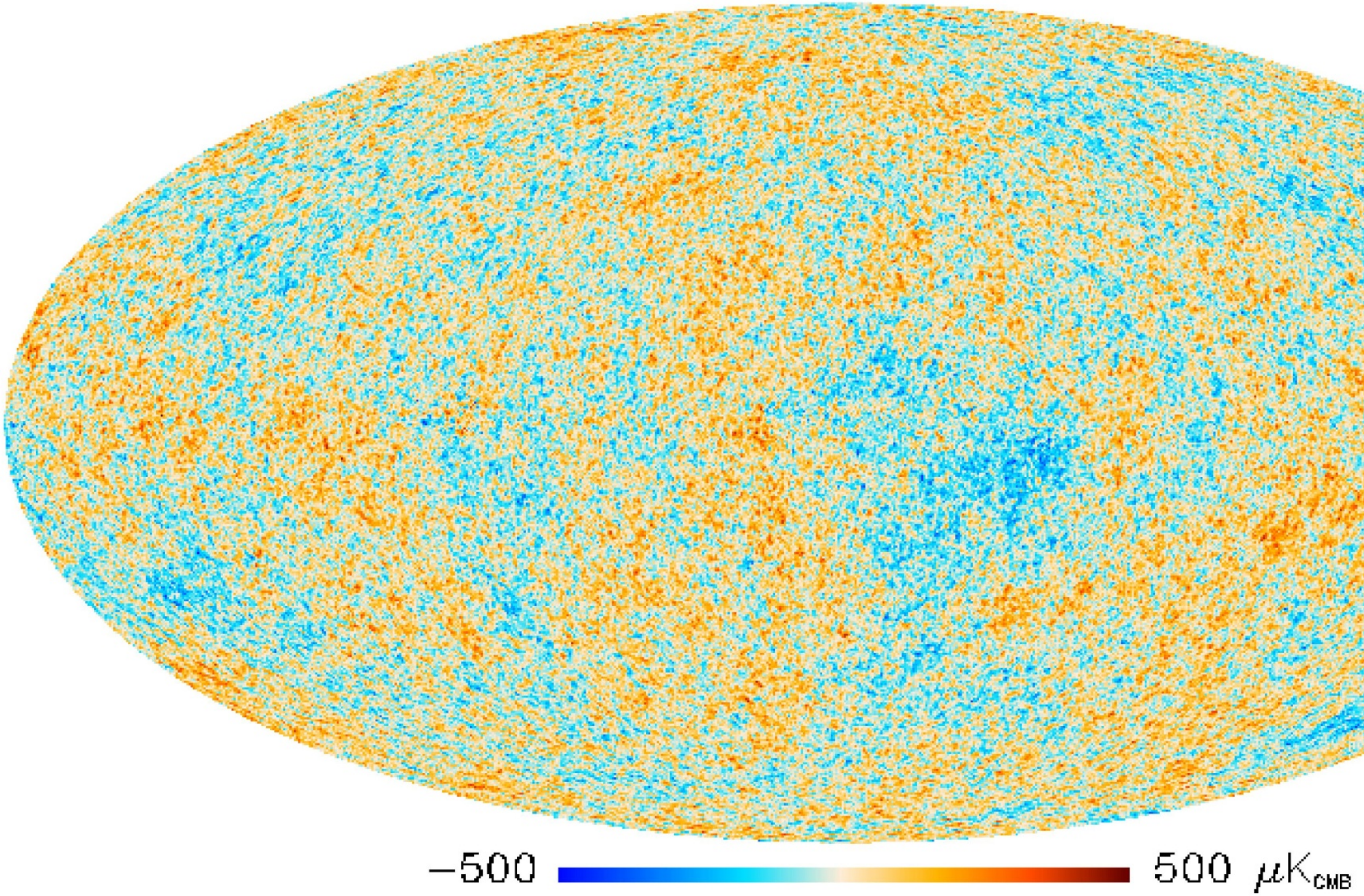

C. Burigana, Paris, Chalonge 2014

APS DEPENDENCE ON COSMOLOGICAL PARAMETERS

***Planck*: a single experiment spanning a wide multipole range!**

Theta → first peak position

Baryon Density → height difference between even and odd peaks

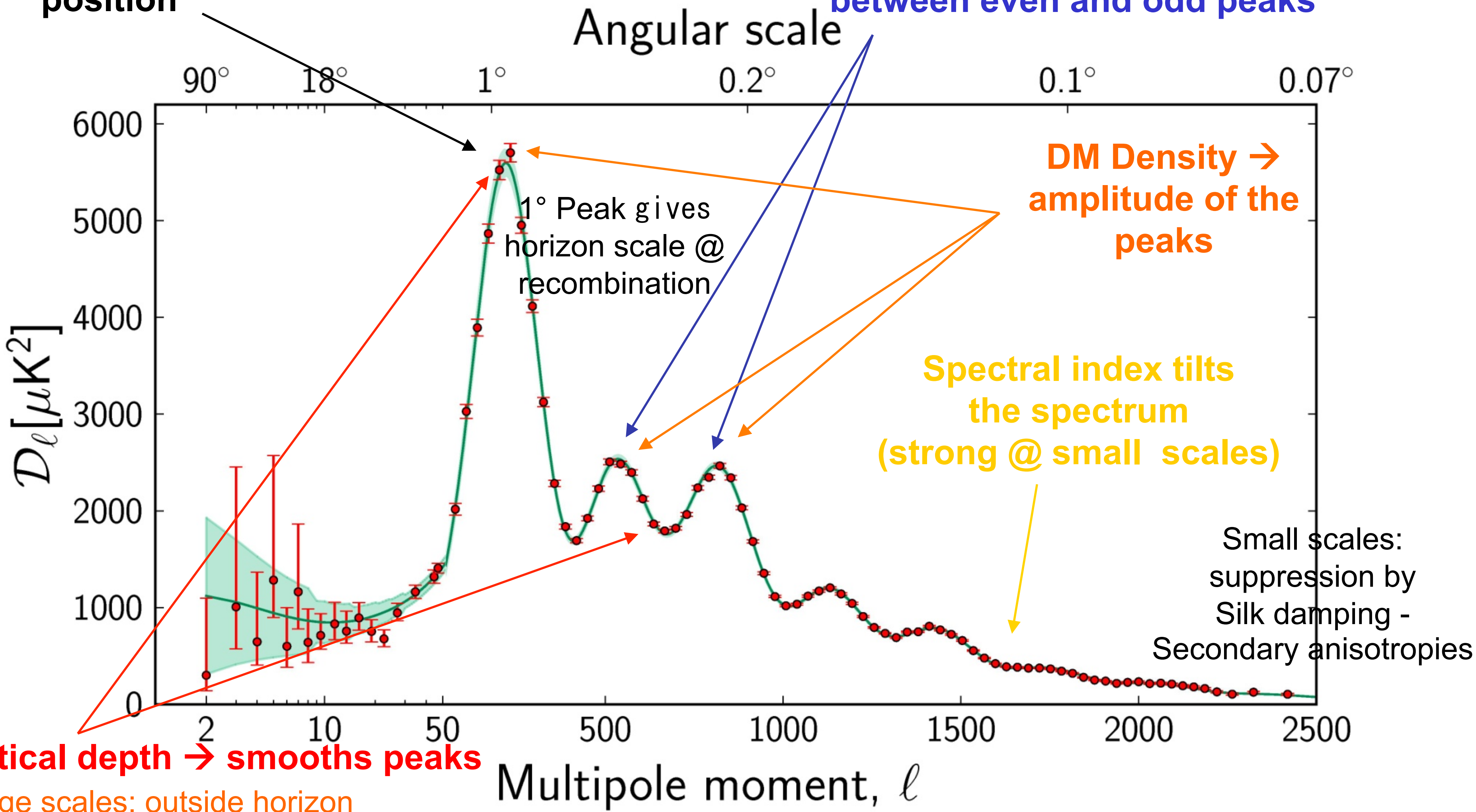

Optical depth → smooths peaks

Large scales: outside horizon @ recombination – only gravity

Intermediate scales: photon-baryon fluid acoustic oscillations - DM potential well vs radiation pressure

C. Burigana, Paris, Chalonge 2014

PLANCK COSMOLOGICAL PARAMETERS: ΛCDM model

	Planck+WP		*Planck*+WP+highL		*Planck*+lensing+WP+highL		*Planck*+WP+highL+BAO	
Parameter	Best fit	68% limits	Best fit	68% limits	Best fit	68% limits	Best fit	68% limits
$\Omega_b h^2$	0.022032	0.02205 ± 0.00028	0.022069	0.02207 ± 0.00027	0.022199	0.02218 ± 0.00026	0.022161	0.02214 ± 0.00024
$\Omega_c h^2$	0.12038	0.1199 ± 0.0027	0.12025	0.1198 ± 0.0026	0.11847	0.1186 ± 0.0022	0.11889	0.1187 ± 0.0017
$100\theta_{MC}$	1.04119	1.04131 ± 0.00063	1.04130	1.04132 ± 0.00063	1.04146	1.04144 ± 0.00061	1.04148	1.04147 ± 0.00056
τ	0.0925	$0.089^{+0.012}_{-0.014}$	0.0927	$0.091^{+0.013}_{-0.014}$	0.0943	$0.090^{+0.013}_{-0.014}$	0.0952	0.092 ± 0.013
n_s	0.9619	0.9603 ± 0.0073	0.9582	0.9585 ± 0.0070	0.9624	0.9614 ± 0.0063	0.9611	0.9608 ± 0.0054
$\ln(10^{10} A_s)$	3.0980	$3.089^{+0.024}_{-0.027}$	3.0959	3.090 ± 0.025	3.0947	3.087 ± 0.024	3.0973	3.091 ± 0.025
Ω_Λ	0.6817	$0.685^{+0.018}_{-0.016}$	0.6830	$0.685^{+0.017}_{-0.016}$	0.6939	0.693 ± 0.013	0.6914	0.692 ± 0.010
σ_8	0.8347	0.829 ± 0.012	0.8322	0.828 ± 0.012	0.8271	0.8233 ± 0.0097	0.8288	0.826 ± 0.012
z_{re}	11.37	11.1 ± 1.1	11.38	11.1 ± 1.1	11.42	11.1 ± 1.1	11.52	11.3 ± 1.1
H_0	67.04	67.3 ± 1.2	67.15	67.3 ± 1.2	67.94	67.9 ± 1.0	67.77	67.80 ± 0.77
Age/Gyr	13.8242	13.817 ± 0.048	13.8170	13.813 ± 0.047	13.7914	13.794 ± 0.044	13.7965	13.798 ± 0.037
$100\theta_*$	1.04136	1.04147 ± 0.00062	1.04146	1.04148 ± 0.00062	1.04161	1.04159 ± 0.00060	1.04163	1.04162 ± 0.00056
r_{drag}	147.36	147.49 ± 0.59	147.35	147.47 ± 0.59	147.68	147.67 ± 0.50	147.611	147.68 ± 0.45

CMB after *Planck* satellite

- **Polarization anisotropy (ground & balloon, space missions):**
  - E mode; TE mode:
  very accurate measures
  - B mode: detection / accurate measures

- **Spectral distortions (ground & balloon, space missions):**
  - Early & late processes:
  detection / measures

- **Very small scales (ground):**
  - Secondary anisotropies / foregrounds
  - Statistical studies
  - Detailed mapping
  → SKA will observe the very long wavelength tail of these CMB related themes

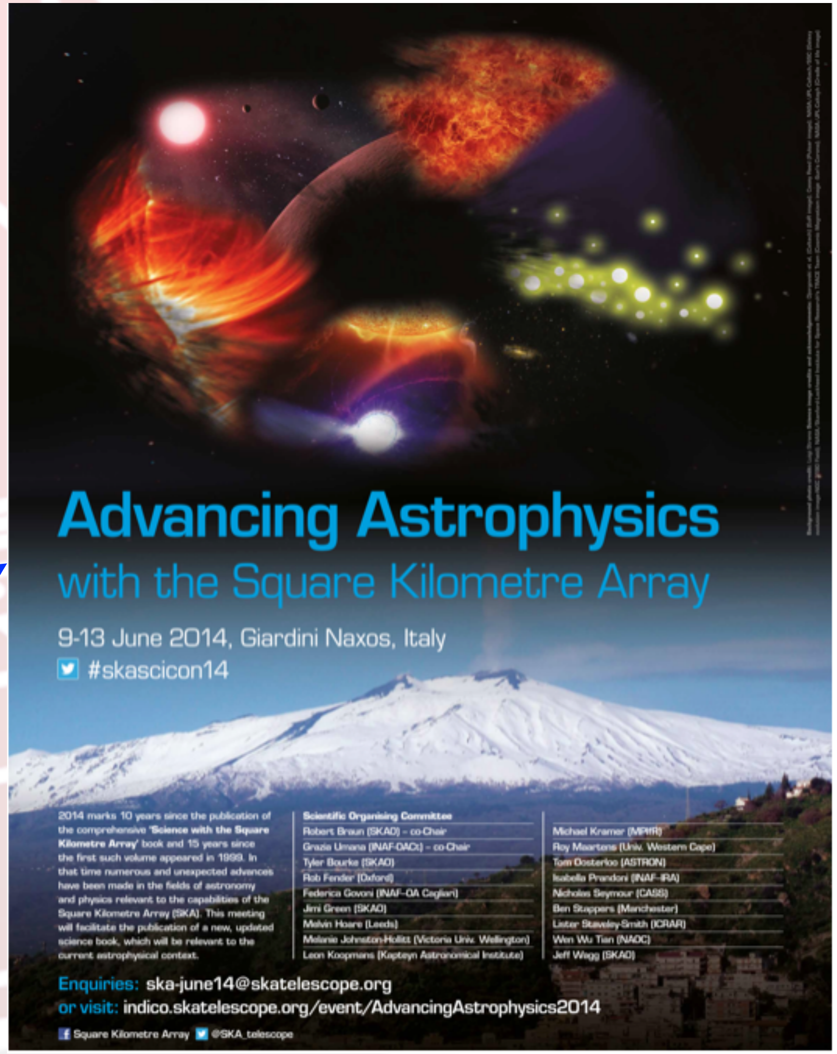

SKA CONCEPT

The collecting area of 10^6 m^2 will be distributed over a number of stations, perhaps as many as ~ 1000.
Each station will have a diameter of 30 - 300 m

The array must be FLEXIBLE → SCALE-FREE
CORE - CONDENSED

The SKA location must be a place allowing the distribution of the antenna over > 1000 km and with a low-level radio-frequency interference

Scientific goals will drive the array design

Courtesy L. Feretti

Countries: Australia, Canada, China, Germany, Italy, Netherlands, New Zealand, South Africa, Sweden, UK, India (info by P. Diamond).
Chapers leaders from: USA, Spain, France, Japan, Portugal, Korea, Taiwan, Croatia (info by R. Braun).

SKA science themes

Mapping: 2004 to 2014

KSP 2004

- Cradle of life
- Strong fields test of gravity using pulsars
- Origin, Evol. Cosmic Magnetism
- Galaxy evolution, Cosmology, Dark Energy
- Probing Dark Ages

SWG 2014

- Cradle of Life
- Pulsars
- Cosmic Magnetism
- Continuum surveys
- HI science
- Cosmology
- Cosmic Dawn/ Reionization
- Time Domain

Courtesy C. Carilli

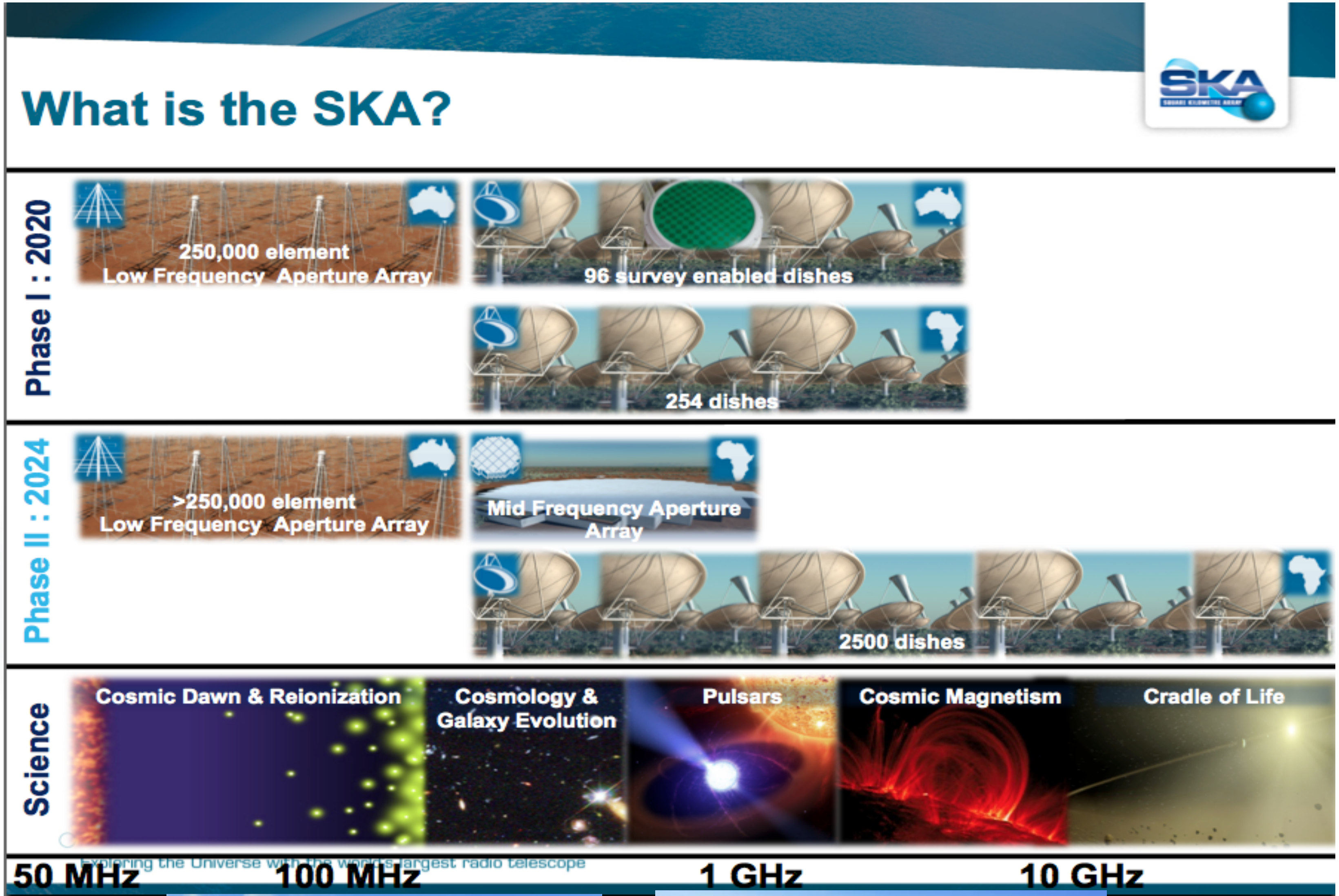

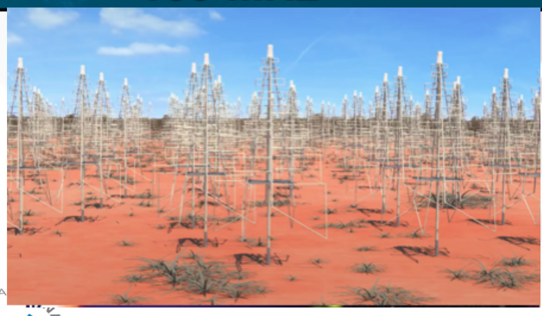

Courtesy
R. Braun

SKA Phase 1

2 sites (South Africa, Australia);
3 telescopes; one Observatory
Frequency range SKA1: 50 MHz – 3 GHz

Cost-cap: €650M
Construction: 2017 – 2023
Early science: 2020
Phase 2 SKA: 2023 - 2030

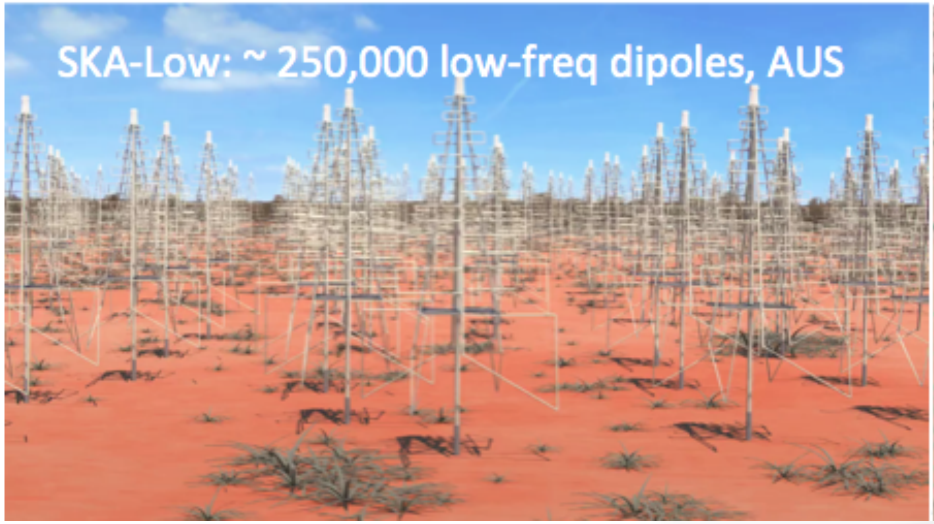

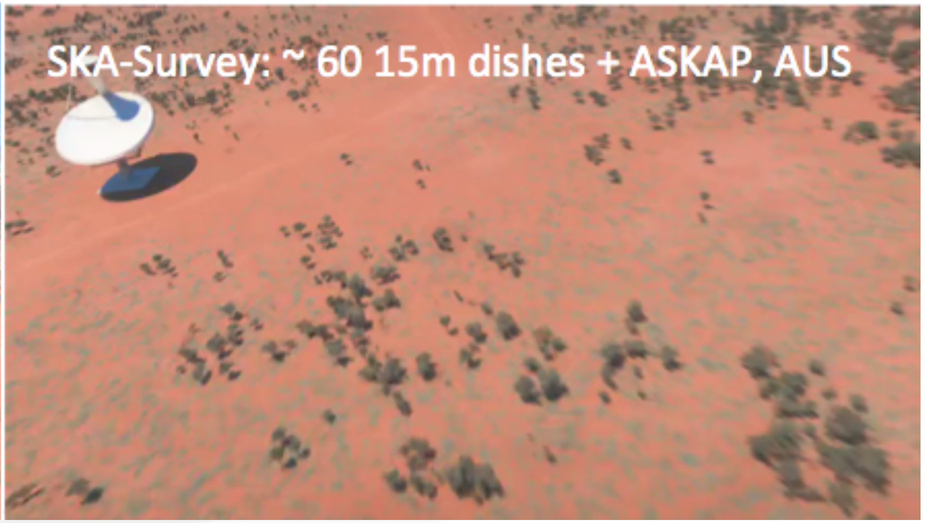

Courtesy P. Diamond

Italian WP & WB

LOFAR also as a precursor

AN ITALIAN SCIENCE CASE FOR LOFAR

Coordinated by :
Gianfranco Brunetti[1]

Contributions by :
Enzo Branchini[2], Gianfranco Brunetti[1], Carlo Burigana[3], Ettore Carretti[1], Rossella Cassano[1], Daniela Crociani[4], Luigina Feretti[1], Andrea Ferrara[5], Marcello Giroletti[1], Karl-H. Mack[1], Mauro Messerotti[6], Lauro Moscardini[4], Matteo Murgia[7], Andrea Possenti[7], Isabella Prandoni[1], Tiziana Venturi[1], Matteo Viel[6]

Italian SKA White Book

June 28, 2013

Endorsed by INAF Scientific Council

Editors[1] & Contributors:

L. Feretti[1], I. Prandoni[1], G. Brunetti[1], C. Burigana[2,35], A. Capetti[3], M. Della Valle[4], A. Ferrara[5], G. Ghirlanda[6], F. Govoni[7], S. Molinari[8], A. Possenti[7], R. Scaramella[9], L. Testi[10,11], P. Tozzi[11], G. Umana[12], A. Wolter[13]

Other Contributors:

L. Amati[2], C. Baccigalupi[14], M.T. Beltrán[11], G. Bonnoli[6], S. Borgani[15,16,17], E. Branchini[18], J.R. Brucato[11], C. Buemi[12], Z.-Y. Cai[15], S. Campana[6], S. Capozziello[19,20], V. Casasola[1], P. Caselli[21,11], R. Cassano[1], P. Castangia[7], , C. Ceccarelli[22,11], R. Cesaroni[11], C. Codella[11], L. Costamante[23], S. Covino[6], G. Cresci[24], P. D'Avanzo[6], M. De Laurentis[19,20], G. De Lucia[15], A. De Rosa[2], G. de Zotti[25], I. Donnarumma[8,31], S. Ettori[24], M. Feroci[8,36], F. Finelli[2], F. Fontani[11], F. Fraternali[26], F. Gastaldello[27], G. Ghisellini[6], G. Giovannini[26,1], M. Giroletti[1], M. Gitti[26,24], A. Gruppuso[2], D. Guidetti[1], L. Guzzo[6], L. Hunt[11], P. Leto[1], C. Maccone[28], M. Magliocchetti[8], F. Mannucci[11], A. Marconi[29], M. Massardi[1], S. Matarrese[30], P. Mazzotta[31], A. Melandri[6], A. Melchiorri[32], N. Menci[9], A. Mesinger[5], M. Murgia[7], M. Negrello[25], M.E. Palumbo[12], F. Panessa[8], D. Paoletti[2], P. Parma[1], F. Perrotta[16], C. M. Raiteri[3], E. M. Rossi[33], A. C. Ruggeri[19,20], R. Salvaterra[27], L. Stella[9], G. Tagliaferri[6], F. Tavecchio[6], A. Tarchi[7], A. Tramacere[34], C. Trigilio[12], G. Trinchieri[13], T. Trombetti[2], S. Turriziani[31], V. Vacca[1], T. Venturi[1], D. Vergani[2], M. Viel[16,17], L. Zampieri[25]

Table A.1. Technical specifications for SKA Precursors, SKA Phase 1 and SKA Phase 2.

Telescope:	ASKAP (2016[a])	Meerkat 1 (2016)	Meerkat 2 (2018)	SKA 1 Low	SKA 1 Mid	SKA 1 AIP–Survey	SKA 2 Low	SKA 2 Mid–Dish	SKA 2 AIP–AA	SKA 2 AIP–PAF
Collector Type:	12m dish	13.5m dish	13.5m dish	Sparse AA	15m dish	15m dish + PAF	Sparse AA	15m dish	Dense AA	15m dish + PAF
No of Collectors:	36	64	64+7	280	250	96	280	2500	280	2000
Frequency Range (GHz):	0.7–1.8	0.9–1.7	0.58–1.7 8.0–14.5	0.07–0.45	0.45–3.0	0.7–1.8	0.07–0.45	0.45–10.0	0.4–1.4	0.45–3.0
Max Bandwidth (GHz):	0.3	0.75		0.38	1.5	0.3	0.38	Depends on feeds	1.0	0.3
< 1 GHz			0.435							
1–1.7 GHz			0.75							
> 8 GHz			2 or 4							
Effective FoV (deg^2):	30	1.0				30	200			
0.5/0.6 GHz			5.6							144
1 GHz			1.9		1.0			1.0		36
1.7/2 GHz			0.62							9
8 GHz			0.03							
14 GHz			0.01							
Sensitivity[b] (m^2/K):	65	> 220				275		10000		
> 90 MHz							4000			
131 MHz				1515						
300 MHz				889						
< 1.2 GHz									10000	
0.45–1.4 GHz					773					
0.6–1.7 GHz			> 220							
1.4 GHz									5000	
1–2 GHz					1031					7000
8–14.5 GHz			> 200							
Telescope Configuration:						TBD				TBD
< 700 m	83%									
700 m – 6 km	17%									
< 1 km		70%	63%	50%	50%		30%	20%	30%	
1 – 5 km				20%	20%		36%	30%	36%	
1 – 8 km		30%	27%							
8 – 16 km			10%							
5 – 100/180 km				30%	30%		34%	30%	34%	
< 180 km								20%		

[a] First observations with ASKAP will be possible from 2014 with a limited number of antennas.

[b] Sensitivity defined as A/T, where A = total collecting area, $T = T_{sys}/\eta$, and η is the aperture efficiency.

Precursor progress: MeerKAT

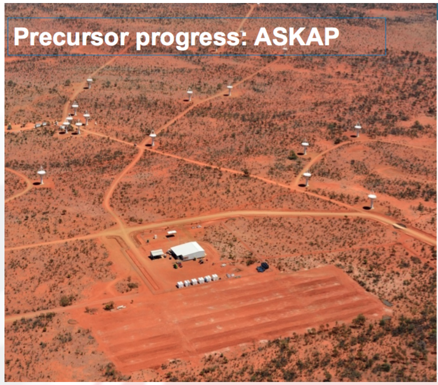

SKA Precursor: Murchison Widefield Array

← LOFAR →

Table A.2. ASKAP indicative sensitivities (for 1^h observation) and survey speeds for different angular resolutions (obtained assuming T_{sys} = 50 K and aperture efficiency $\eta = 0.8$).

Parameter	10"	18"	30"	90"	180"	Units
Continuum Sensitivity (300 MHz)	37	29	34	74	132	μJy/beam
Line Sensitivity (100 kHz)	2.1	1.6	1.9	4.1	7.3	mJy/beam
Surface Brightness Sensitivity (5 kHz)	–	–	5.2	1.3	0.56	K
Continuum Survey Speed (300 MHz, 100 μJy)	220	361	267	54	17	deg^2/hr
Line Survey Speed (100 kHz, 5 mJy)	184	301	223	45	14	deg^2/hr
Surface Brightness Survey Speed (5 kHz, 1 K)	–	–	1.1	18	94	deg^2/hr

SKA & CMB: enthusiasm → discouragement → realism! → enthusiasm!

SKA ROLE to THE SUBJECT OF THIS PRESENTATION

CONTRIBUTIONS OF SKA ALONE?

Subrahmanyan R., Ekers R.D., 2002, in the XXVIIth General Assembly of the URSI, August 17-24, Maastricht, The Netherlands, astro-ph/0209569

CONTRIBUTIONS OF SKA ALONE VS DEDICATED PROJECTS?

CMB experiments, Ryle Telescope (13m antennas, 15GHz), OVRO interferometer (10m antennas, 30GHz), BIMA array (6m antennas, 30GHz), AMI, SZA (antennas $\sim$ few $\times$ 100λ), ALMA ($\simeq$ PLANCK ν coverage, SKA resolution)

Jones M.E., 2003, in *The scientific promise of the Square Kilometer Array*, SKA Workshop, Oxford, 7 November 2002, eds. Kramer M., Rawlings S., pg. 47,

http://www.skatelescope.org/documents/

Workshop_Oxford2002.pdf

CONTRIBUTIONS OF SKA IN THE CONTEXT OF NEXT DECADE(S) PROJECTS?

This work

Sunyaev–Zeldovich effects, free–free emission, and imprints on the cosmic microwave background, New Astronomy Reviews 48 (2004) 1107–1117, in **Science with the Square Kilometre Array**

Outline

- ✧ SKA science … from the point of view of the synergies with CMB/microwave surveys with reference to Italian WB
  - ✧ In “3 Cosmology - 3.6 Synergy with CMB projects”
    - ✧ SZ from clusters
    - ✧ SZ @ galaxy scales
    - ✧ Implications for CMB spectrum studies
    - ✧ Cross-correlations CMB ←→ RS catalogues
    - ✧ Free-free signals @ various epochs ←→ reionization
  - ✧ In “6 Galaxy Clusters and Magnetic Fields - 6.2 Magnetic Fields”
    - ✧ Primordial Magnetic Fields
  - ✧ In “8 Interstellar Medium, Solar System, Planetary Science, Bioastronomy”
    - ✧ 8.3 Galactic foregrounds versus Galactic astronomy

Some References

[1] Sunyaev R.A., Zeldovich Ya.B., 1972, Comm. Astrophys. Space Phys., 4, 173
[2] Rephaeli Y., 1995, ARA&A, 33, 541
[3] Rees M.J., Ostriker J.P., 1977, MNRAS, 179, 541
[4] White S.D.M., Rees M.J., 1978, MNRAS, 183, 341
[5] Ikeuchi S., 1981, PASJ, 33, 211
[6] Platania P., Burigana C., De Zotti G., Lazzaro E., Bersanelli M., 2002, MNRAS, 337, 242
[7] Lapi A., Cavaliere A., De Zotti G., 2003, ApJ, 597, L93
[8] Burigana C., de Zotti G., Feretti L., 2004, New Astronomy Reviews, 48, 1107
[9] Pei Y.,1995, ApJ, 438, 623
[10] Oh S.P., 1999, ApJ, 527, 16
[11] Partridge R.B., Richards E.A., Fomalont E.B., Kllerman K.I., Windhorst R., 1997 ApJ, 483, 38
[12] Ponente P.P., Diego J.M., Sheth R.K., Burigana C., Knollmann S.R., Ascasibar Y., 2011, MNRAS, 410, 2353
[13] Trombetti T., Burigana C., 2013, will appear on MNRAS
[14] Feretti L., et al., Italian SKA White Book, 2013
[15] Tegmark M., 1997, Phys. Rev. D, 55, 5895
[16] Sachs R.K., Wolfe A.M., 1967, ApJ, 147, 73
[17] Crittenden R.G., Turok N., 1996, Physical Review Letters, 76, 575
[18] Raccanelli A., Bonaldi A., Negrello M., et al. 2008,MNRAS, 386, 2161
[19] Schiavon F., Finelli F., Gruppuso A., et al., 2012, MNRAS, 427, 3044
[20] Xia J.Q., Baccigalupi C., Matarrese S., Verde L., Viel M., 2011, JCAP, 08, 033
[21] Ryu D., Schleicher D.R.G., Treumann R.A., Tsagas C.G., Widrow L.M., 2012, Space Sci. Rev., 166, 1
[22] Widrow L.M., Ryu D., Schleicher D.R.G., et al., 2012, Space Sci. Rev., 166, 37
[23] Paoletti D., Finelli F., 2011, Phys. Rev. D, 83, 123533
[24] Caprini C., Finelli F., Paoletti D., Riotto A., 2009, JCAP, 6, 21
[25] Neronov A., Vovk I., 2010, Science, 328, 5974 73
[26] Burigana C., La Porta L., Reich P., Reich W., 2006, AN, 327, 491
[27] Bennett C.L., Larson D., Weiland J.L., et al., 2013, ApJS, submitted, arXiv:1212.5225

Slide from Francois Bouchet

Inflation has a few variants…

planck

- assisted brane inflation
- anomaly-induced inflation
- assisted inflation
- assisted chaotic inflation
- B-inflation
- boundary inflation
- brane inflation
- brane-assisted inflation
- brane gas inflation
- brane-antibrane inflation
- braneworld inflation
- Brans-Dicke chaotic inflation
- Brans-Dicke inflation
- bulky brane inflation
- chaotic inflation
- chaotic hybrid inflation
- chaotic new inflation
- Chromo-Natural Inflation
- D-brane inflation
- D-term inflation
- dilaton-driven inflation
- dilaton-driven brane inflation
- double inflation
- double D-term inflation
- dual inflation
- dynamical inflation
- dynamical SUSY inflation
- 5-dimensional assisted inflation
- eternal inflation
- extended inflation
- extended open inflation
- extended warm inflation
- extra dimensional inflation
- ...

- F-term inflation
- F-term hybrid inflation
- false-vacuum inflation
- false-vacuum chaotic inflation
- fast-roll inflation
- first-order inflation
- gauged inflation
- Ghost inflation
- Hagedorn inflation

- higher-curvature inflation
- hybrid inflation
- Hyper-extended inflation
- induced gravity inflation
- intermediate inflation
- inverted hybrid inflation
- Power-law inflation
- K-inflation
- Super symmetric inflation

- Quintessential inflation
- Roulette inflation
- curvature inflation
- Natural inflation
- Warm natural inflation
- Super inflation
- Super natural inflation
- Thermal inflation
- Discrete inflation
- Polarcap inflation
- Open inflation
- Topological inflation
- Multiple inflation
- Warm inflation
- Stochastic inflation
- Generalised assisted inflation
- Self-sustained inflation
- Graduated inflation
- Local inflation
- Singular inflation
- Slinky inflation
- Locked inflation
- Elastic inflation
- Mixed inflation
- Phantom inflation
- Non-commutative inflation
- Tachyonic inflation
- Tsunami inflation
- Lambda inflation
- Steep inflation
- Oscillating inflation
- Mutated hybrid inflation
- Inhomogeneous inflation
- ...

François R. Bouchet "Planck constraints on fundamental physics" ESLAB, April 2nd, 2013 7

Cosmic Inflation (if any) produces primordial density and tensor perturbations

- **Tensors produce rotational modes (B-modes) in the CMB polarization field**
- **Most inflation models predict a slight level of non-Gaussianity of fluctuations**
- **Dissipation of density fluctuations produces distortions in the CMB spectrum**

Future (we hope!) (ESA) CMB missions:

COrE (or new M idea)
PRISM (L mission)

Now we are working for a new ESA M4 mission (next ESA call)
COrE+

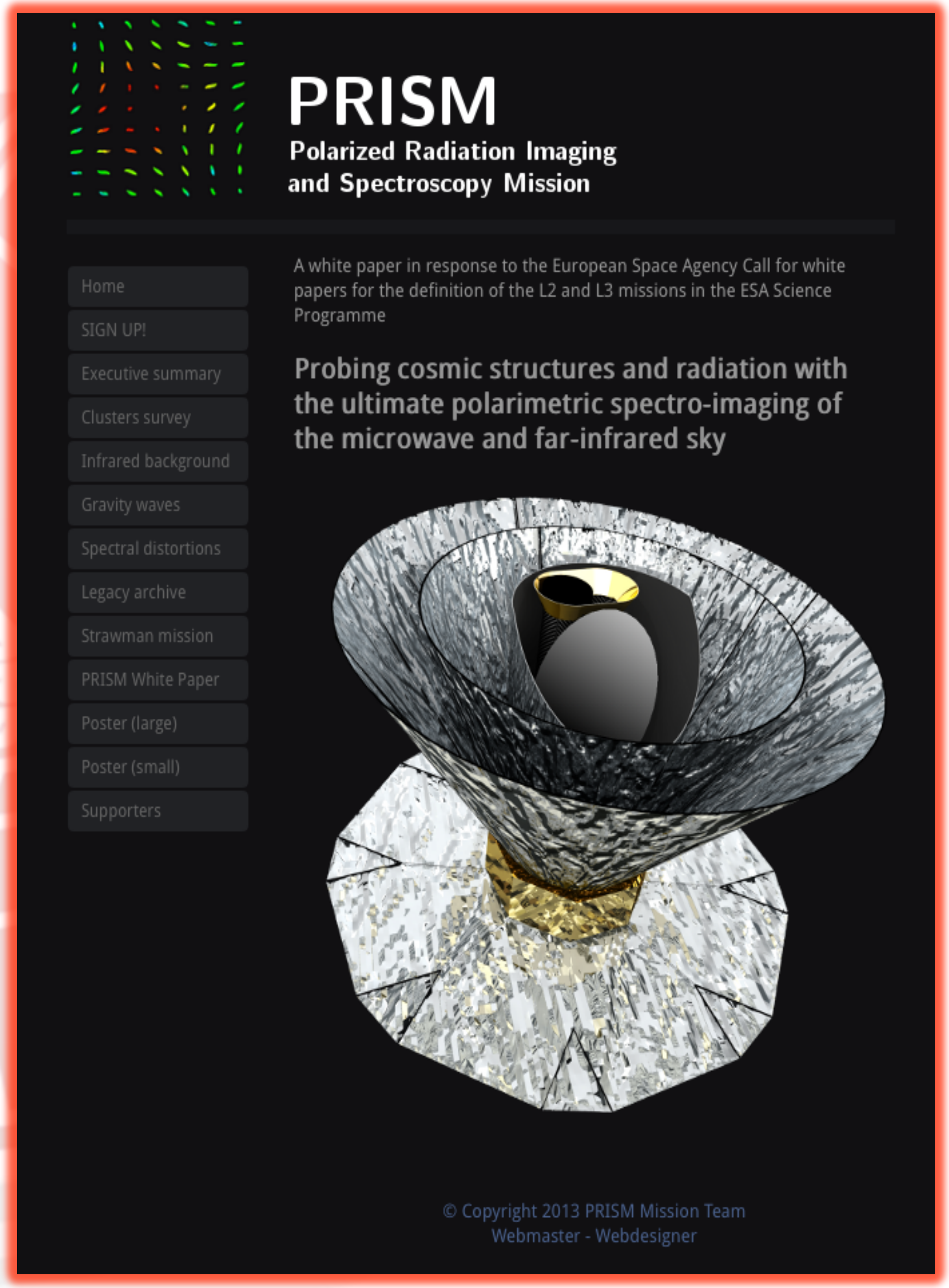

In a nutshell: New science with a polarimetric and spectral survey of the **Hubble volume** from the μ–wave to the far-IR

5 Ultimate measurement of CMB polarization, Gaussianity, and absolute spectrum. Search for the gravitational waves produced during inflation.

1 **Ultimate galaxy cluster survey** via Sunyaev-Zeldovich effect (SZ): ($>10^6$: all clusters with $M>10^{14}M_{\odot}$ within our horizon)

Legacy archive of hundreds of full-sky intensity and polarization maps from tens of GHz to few THz with extreme precision and resolution :
$1\mu K_{CMB}$arcmin
1'FWHM@λ1mm

6 A complete survey of the interstellar medium in the Milky way : dust, molecular lines, magnetic field, …

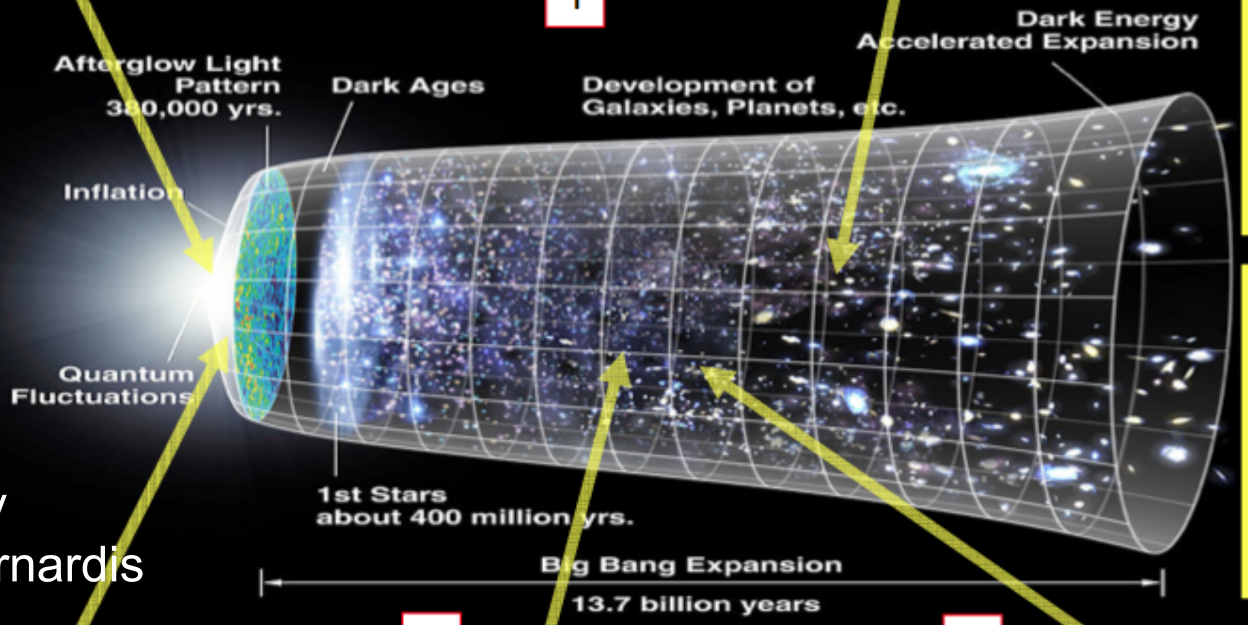

Courtesy P. de Bernardis

4 Probe epochs before recombination and new physics using CMB spectral distortion measurements

3 Map the gravitational potential all the way to z=1100 through CMB lensing

2 Probe early star formation and its evolution through precision characterization of the Cosmic Infrared Background (CIB)

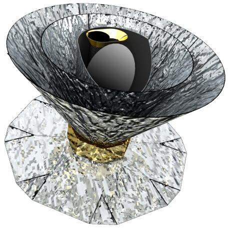

Scientific themes for future microwaves to far-IR missions

- Primordial CMB B-modes, high precision CMB T (absolute!) and E
- CMB spectral distortions
  - thermal history, energy exchanges between CMB and matter
  - reionisation, decaying dark-matter particles, small scale primordial P(k)
- All crucial/unique for → early Universe & fundamental physics

- 3D cosmic structures:
  - A complete census of galaxy clusters (hot baryons and mass up to z>3)
  - CMB lensing (projected mass)
  - The CIB and dusty galaxies (up to z>6) – dust, AGNs and interplay, P(k) in shells
- 3D cosmic velocity flows
- All phases of the galactic interstellar medium:
  - Dust (thermal, spinning, size and chemical composition)
  - Cosmic rays (synchrotron components)
  - Gas (neutral and ionised), free-free, atoms and molecules, molecular clouds,
  - Magnetic field via polarisation of dust (and synchrotron)

CMB polarization with *Planck*
E & B – 30% binning, f_{sky}=74%

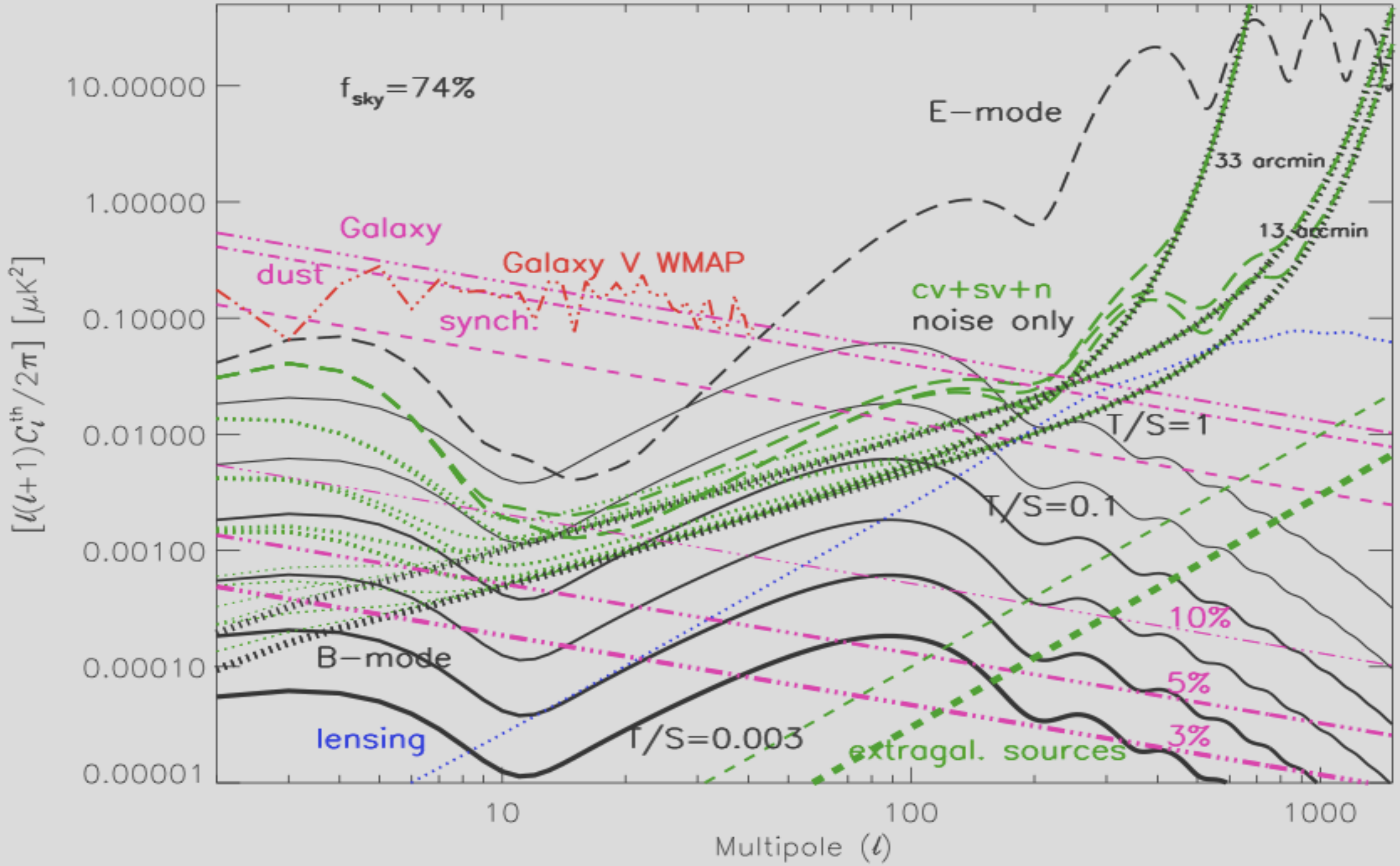

5 Measuring B-modes

- Measuring B-modes to r=0.001 will require **exquisite control of polarized foregrounds**.
- Current extrapolations with the simplest allowed foreground models predict that the galactic foreground will outshine the r=0.001 primordial by about x100 in all frequency channels, and emission properties are likely to be more complicated than many of the optimistic foreground forecasts suggest
- While forthcoming experiments could find hints of cosmological B modes, **only a large mission with wide frequency coverage and high angular resolution can provide a reliable and convincing detection.**

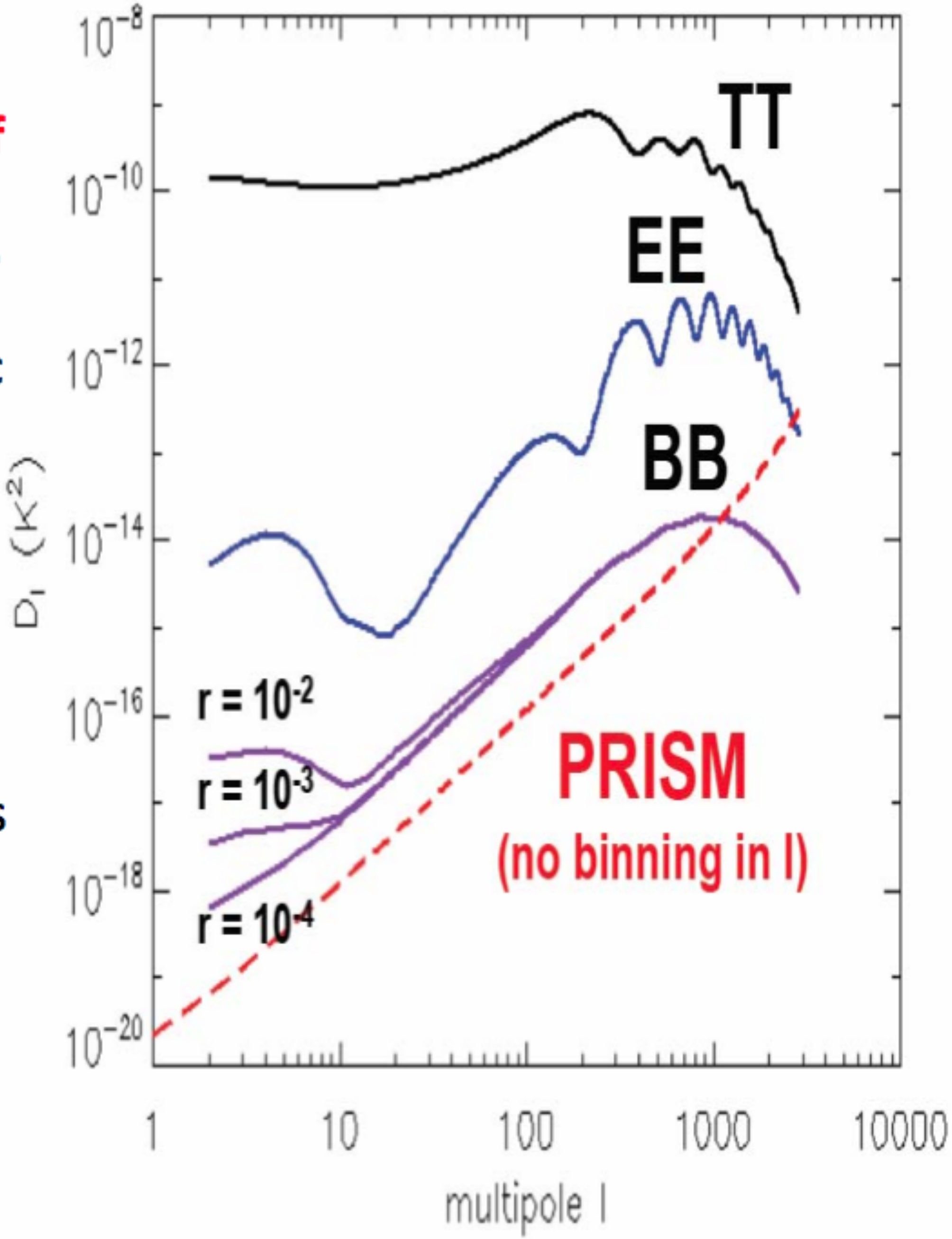

Reionizaton: beyond τ approximation

- The so-called τ or z_{RE} "approximation" in CAMB code for CMB APS computation through numerical solution of Boltzmann equation "implies" a given simple analytical recipe for χ evolution

- More realistic models assume χ evolution based on
  - phenomenological approaches mimicking classes of (astro)physical processes
  - astrophysical models
  - detailed physical processes

Observables vs physical mechanisms

- **Thomson scattering**
  - Anisotropies, mainly
    - EE, BB, TE modes
  - Comptonization distortions

- **Free-free**
  - Distortions (intermediate/long wavelengths)
  - Link with clumping

Astrophysical reionization models

Inhomogeneous reionization: lognorm overdensity distribution.

Sources of reionization:

- PopIII stars: Salpeter IMF but metal free (Schaerer 06)
- PopII stars: Salpeter IMF, Bruzual & Charlot
- Quasars: important for $z<6$

Chemical feedback governs the transition from PopIII to PopII stars ($Z_{crit}=10^{-5+/-1}$ Z_{sun}): the two populations are coeval and PopIII stars can form also at relatively low-z.

Radiative feedback: temperature increase in ionized region → huge suppression of low-mass galaxies formation.

✓**Suppression model** (Choudhury & Ferrara '06, MNRAS, 371, L55): radiative feedback is effective in DM haloes with circular velocity below a critical value $v_{crit} \sim (2k_B T/\mu m_p)^{1/2}$ where T is the average temperature of ionizing regions [~ 30 km/s for $T=3\times10^4$ K]

✓**Filtering model** (Gnedin 2000 ApJ, 542, 535): the average baryonic mass within haloes in photoionized regions is a fraction of the universal value:

$$\frac{M_b}{M} = \frac{\Omega_b / \Omega_m}{[1+(2^{1/3}-1)M_C / M]^3}$$

where M_C is the mass of haloes that retain 50% of their gas mass.

Phenomenological models

(Naselsky & Chiang 04, MNRAS 347, 795)

$$\varepsilon_i(z) = \varepsilon_0 \exp\left[-\frac{(z - z^{(1)}_{\rm reion})^2}{(\Delta z_1)^2}\right] + \varepsilon_1 (1+z)^{-m} \Theta(z^{(1)}_{\rm reion} - z)$$

here ε_0, $z^{(1)}_{\rm reion}$, and $\Delta z_1 \ll z^{(1)}_{\rm reion}$ are free parameters describing the history of the first epoch of reionization which significantly decreases at $z > z^{(1)}_{\rm reion}$; ε_1, m, and (again) $z^{(1)}_{\rm reion}$ are free parameters describing the history o P. Naselsky and L.-Y. Chiang, 2004, MNRAS, 347, 795:reasing of $\varepsilon_i(z)$ with the time, being $\Theta(x)$ the step function.

$$\varepsilon_i(z) = \xi \exp\left[-\frac{(z - z_{\rm reion})^2}{(\Delta z)^2}\right]$$

quite similar to that assumed to describe the first reionization epoch for late processes, can be exploited in this context [37]; again ξ, $z_{\rm reion}$, and Δz are free parameters describing the history of this high redshift reionization scenario. Assuming $\Delta z \ll z_{\rm reion}$ implies the choice of a peak-like model.

Extension to all modes
B-modes & reionization beyond simple tau-approximation

- Future of CMB polarization anisotropies:
  - towards B-modes & full exploitation of all modes
- Implementation of reionization models in CAMB code considering all modes & in particular B-modes (T. Trombetti & C.B., 2012, JMP, 3, 1918)
- Inclusion of
  - Phenomenological models (high/low z)
  - Astrophysical models
  - Mix of models

Typical cases →

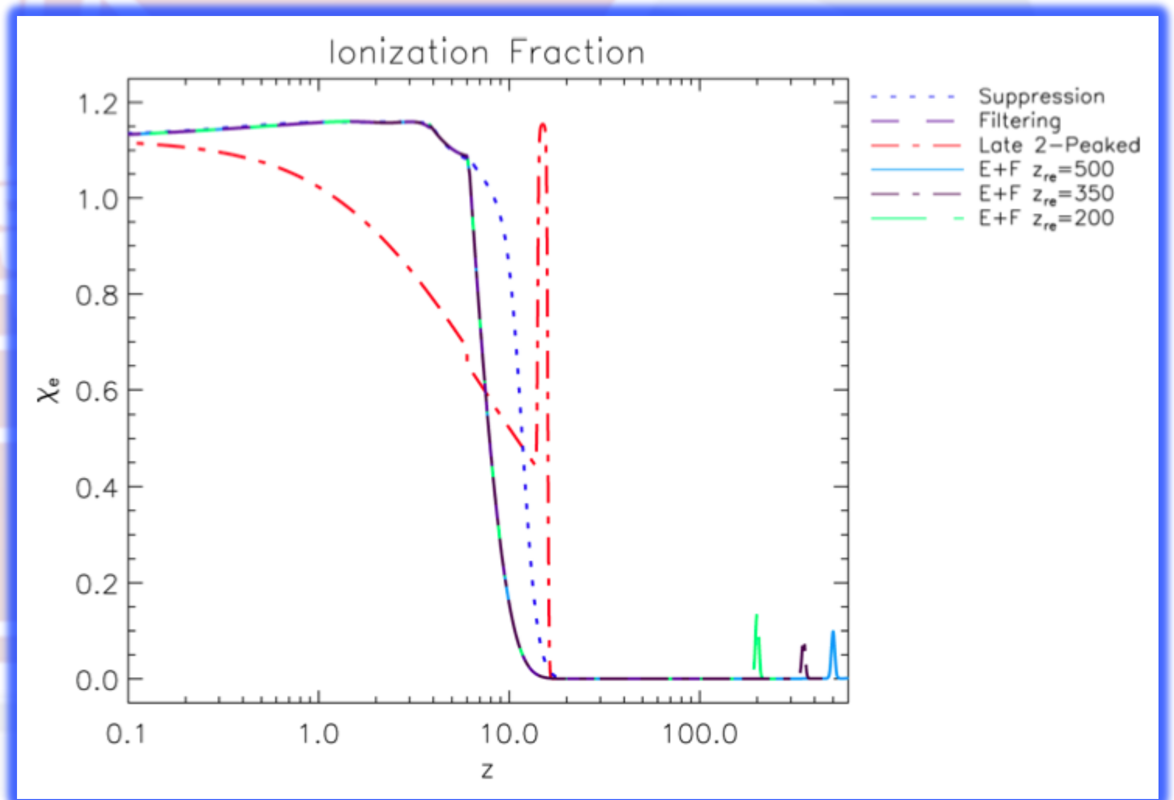

EE & BB predictions

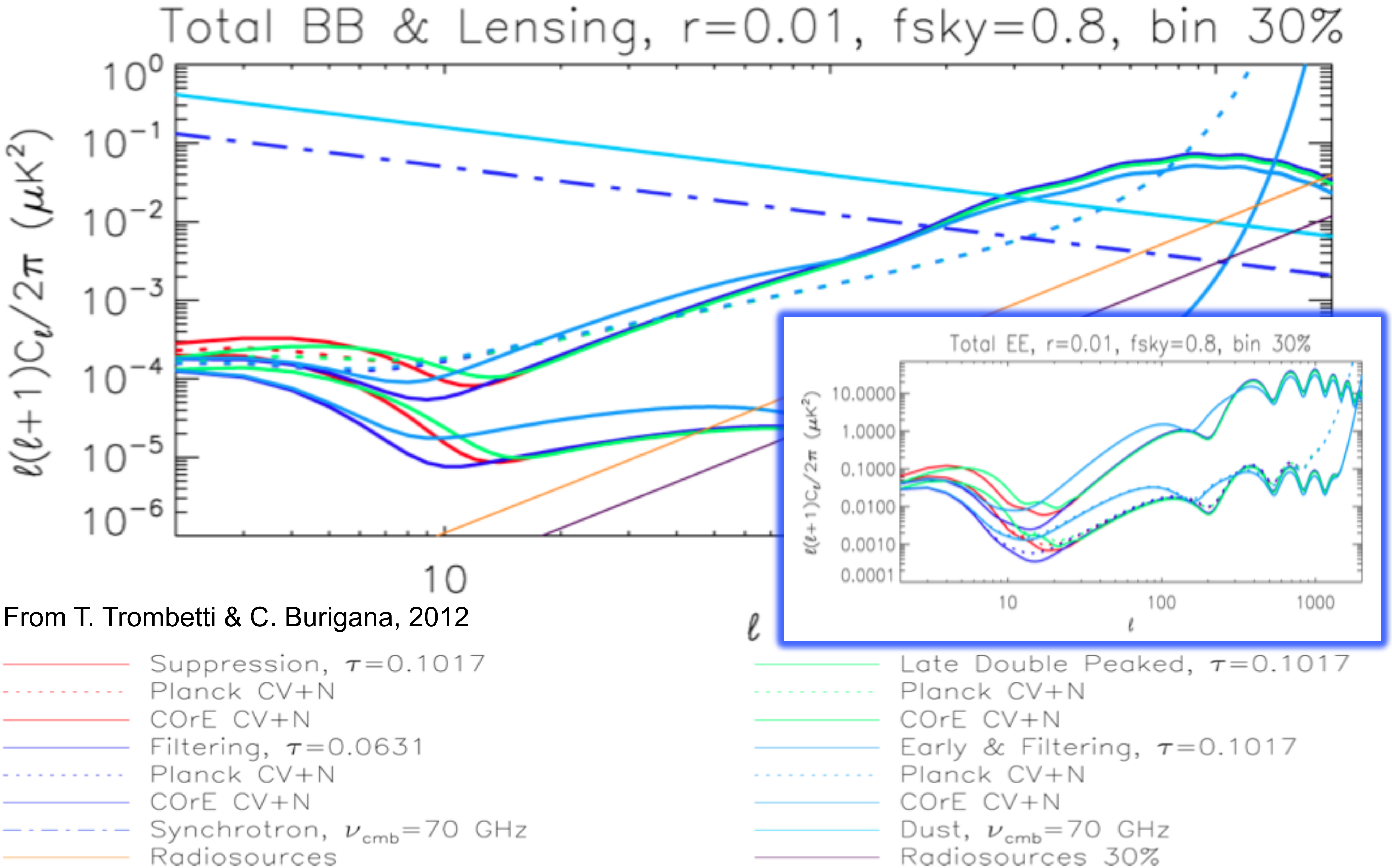

From T. Trombetti & C. Burigana, 2012

Reionization BB: comparing models & experiments

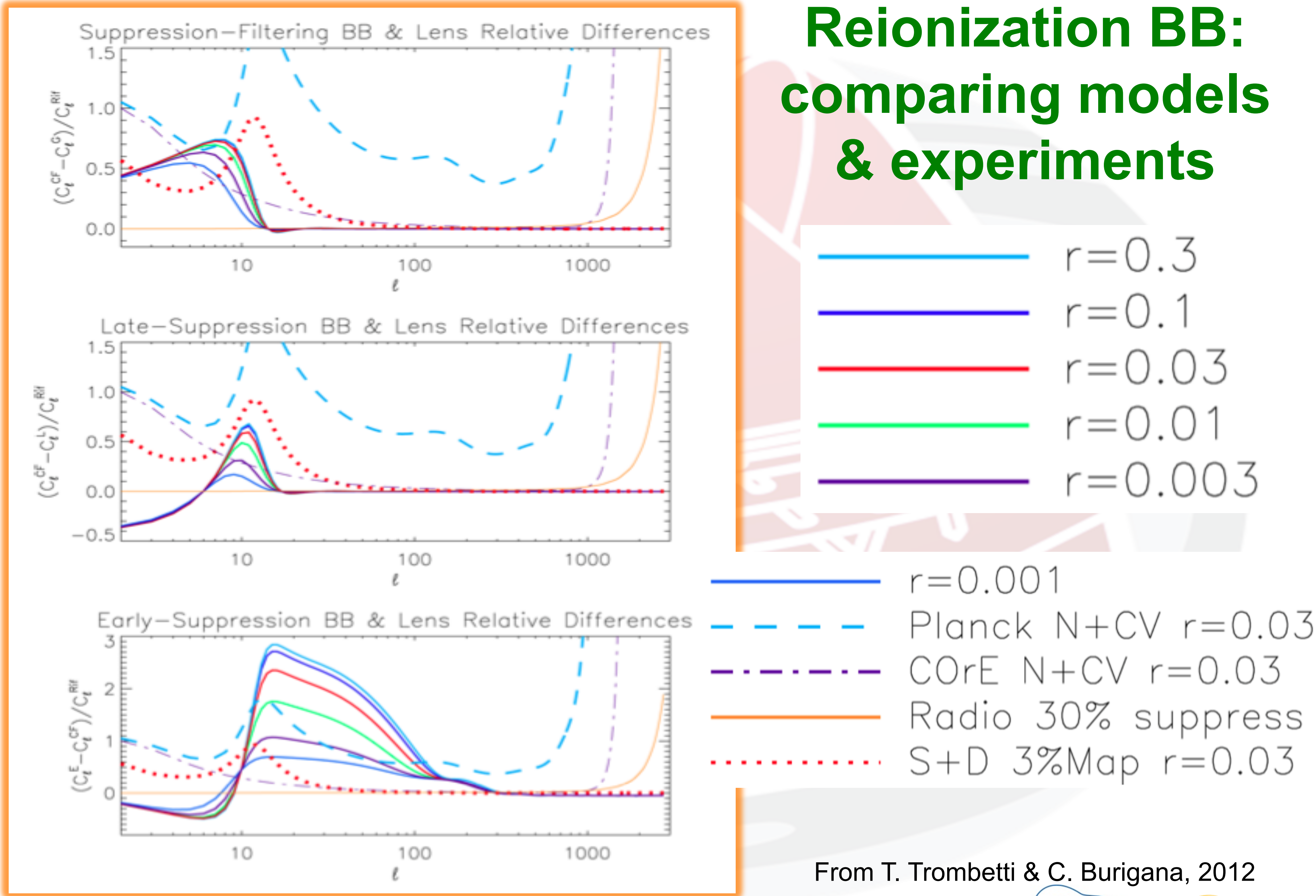

From T. Trombetti & C. Burigana, 2012

Reionization: synergy with all-sky 21cm background signal

Temperatures: [kinetic, CMB spin (21 cm)]

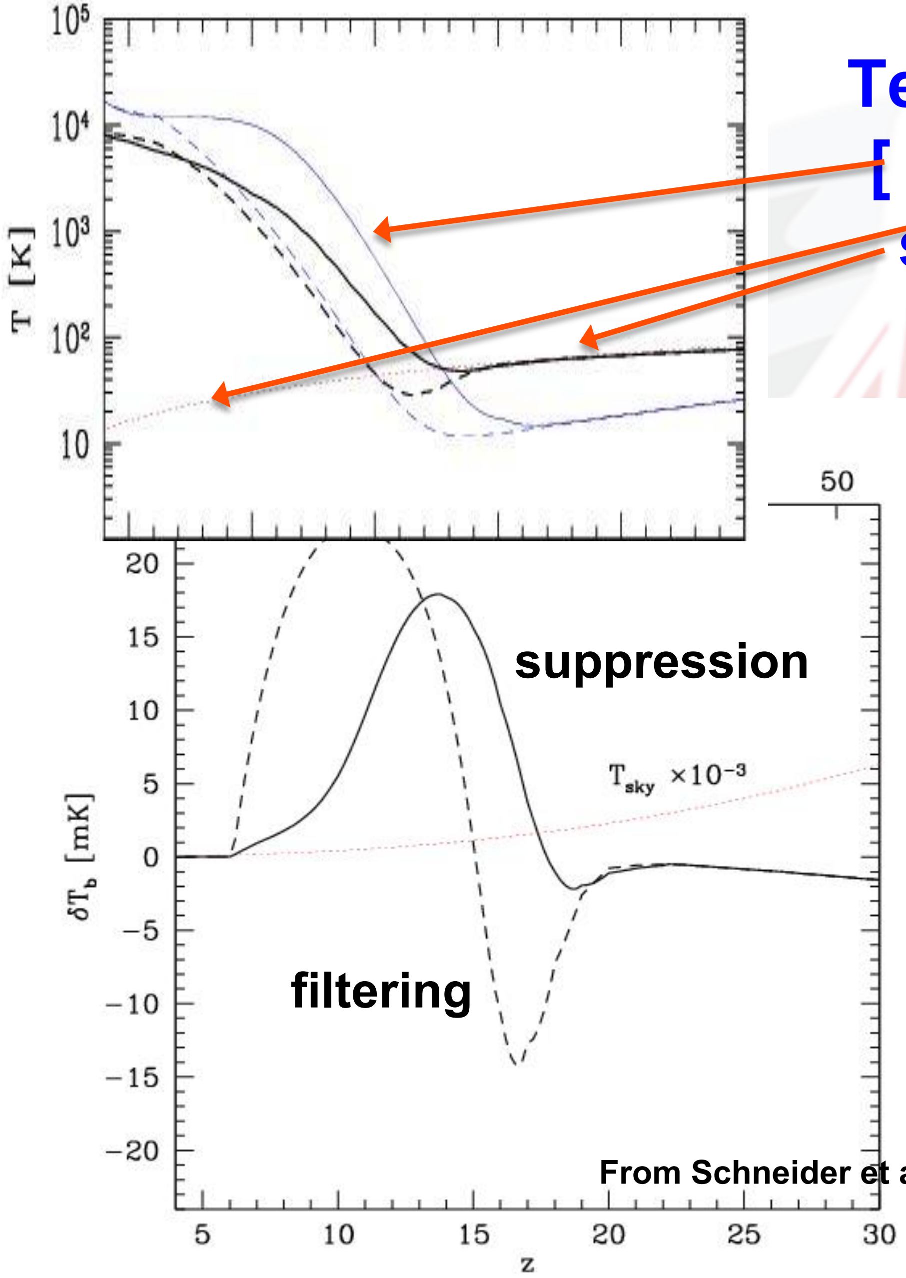

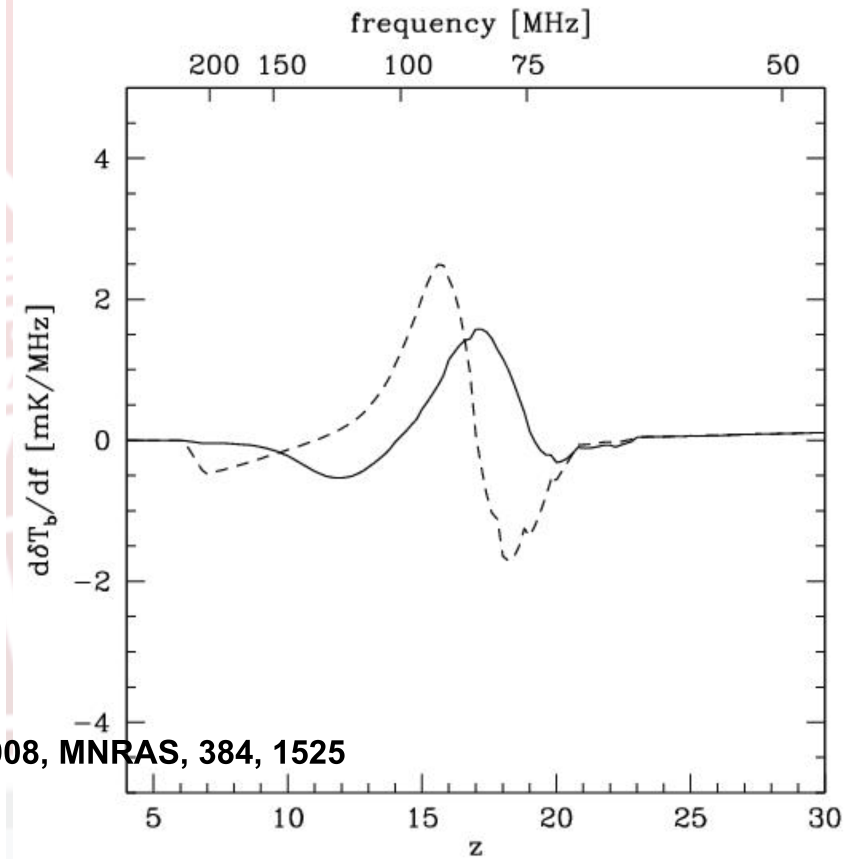

From Schneider et al. 2008, MNRAS, 384, 1525

require removal of foreground at a few x 10^{-3} level

C. Burigana, Paris, Chalonge 2014

21cm signal: distinguishing models

Ex.: filtering - suppression

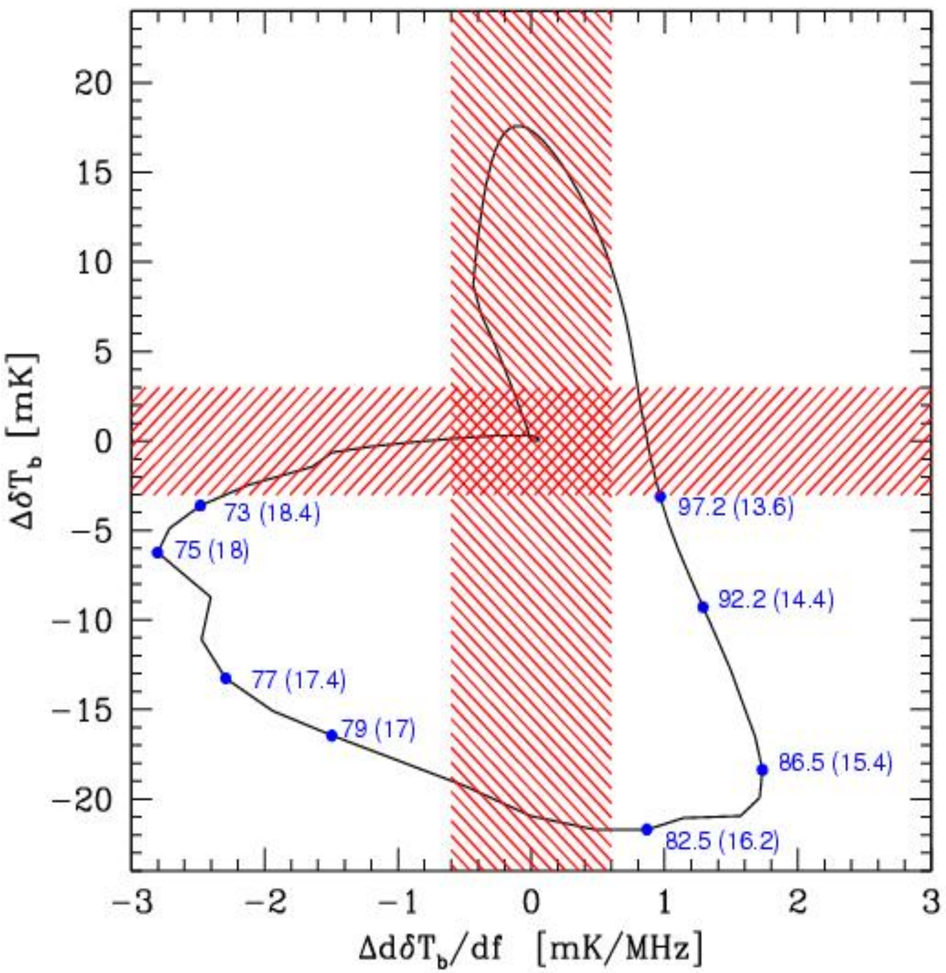

A successful detection requires:

$\Delta\delta T_b > 3$ mK

$\Delta(d\,\delta T_b/df) > 0.6$ mK MHz^{-1}

Single-dish, all sky 21cm observations can discriminate between the two model in the frequency ranges

ν_{obs} = 73-79 MHz (z=17-18.4)

ν_{obs} = 82.5-97.2 MHz (z=13.6-16.2)

From Schneider et al. 2008, MNRAS, 384, 1525

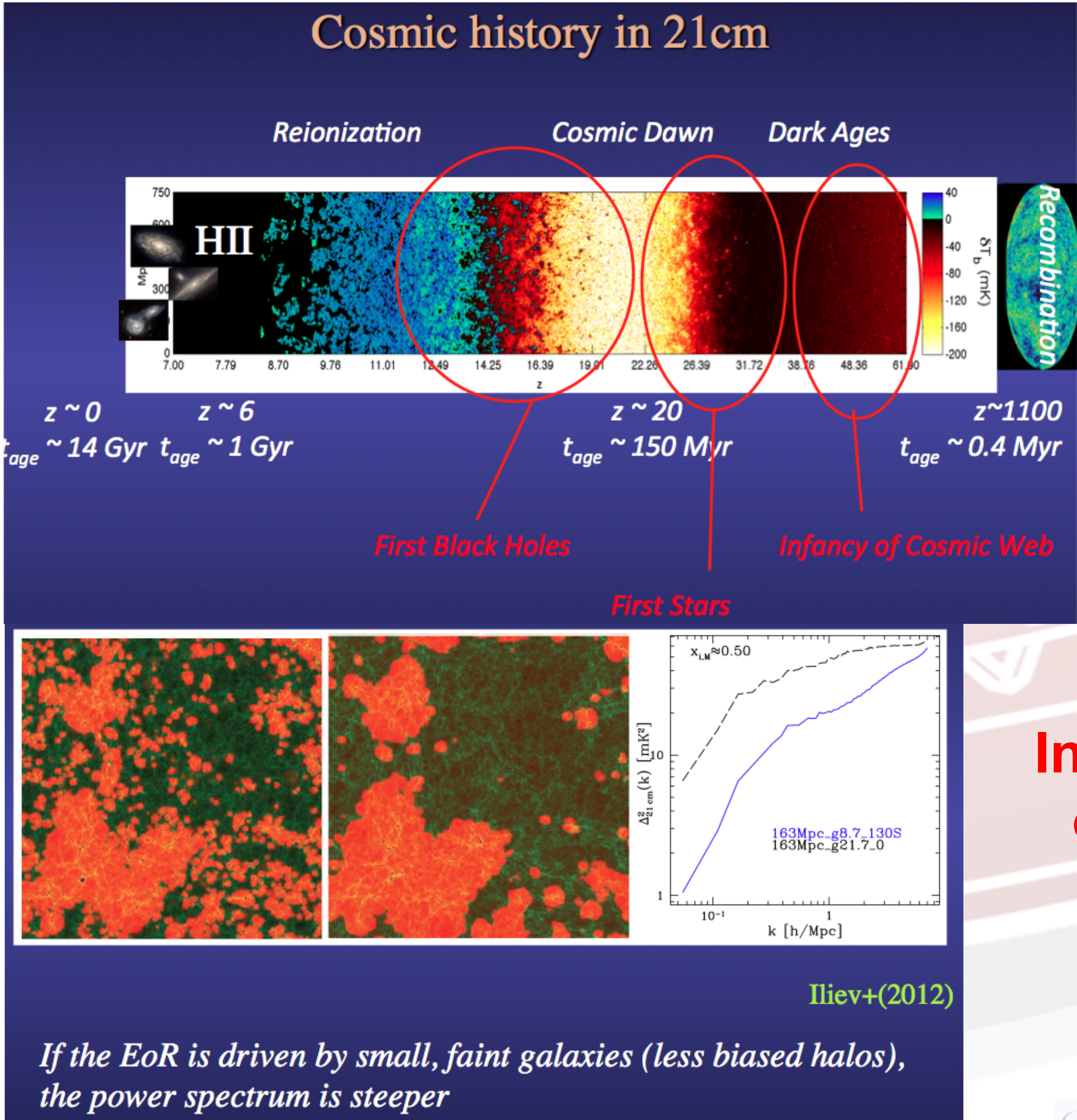

Fluctuations of 21 cm as diagnostic of reionization process

Courtesy
A. Mesinger et al.

Insights on type of sources …

again power spectrum …

Thermal and kinetic Sunyaev-Zeldovich (SZ) effect towards galaxy clusters

The scattering of CMB photons from hot electrons in galaxies and clusters of galaxies produces a frequency dependent change in the CMB brightness (Sunyaev & Zeldovich '72, Rephaeli '95 [1,2]):

- ✧ hot electron gas is globally at rest with respect to the observer → thermal SZ effect
- ✧ bulk peculiar motion, Vr, of the hot electron gas → kinetic SZ effect

In the Rayleigh-Jeans (RJ) region:

- ➢ thermal SZ effect → decrement of the surface brightness towards the cluster
- ➢ kinetic SZ effect → decrement or an increment depending on the direction of the cluster velocity with respect to the observer

They can be separated through multi-frequency observations on a wide frequency range.

Planck 2013 results. XXIX. *Planck* catalogue of Sunyaev–Zeldovich sources

- The catalogue contains **1227 entries**, making it over six times the size of the *Planck* Early SZ (ESZ) sample and the largest SZ-selected deepest all-sky cluster ccatalogue to date.
- It contains **861 confirmed** clusters: 178 have been confirmed as clusters, mostly through follow-ups, and a further 683 are previously-known.
- 366 are cluster candidates: three classes according to the quality of evidence that they are likely to be true clusters.
- z to ≅ 1, broadest **range from (0.1 to 1.6) × 10^{15} $M_\odot$**.
- **Confirmation** of cluster candidates through comparison with existing surveys or cluster catalogues, catalogue statistical characterization in terms of completeness and statistical reliability. **Validation** process through additional information.
- This gives an ensemble of **813 cluster redshifts**, and for all these *Planck* clusters we also include a **mass** estimated from a newly-proposed SZ-mass proxy.
- Refined measure of the **SZ Compton parameter** for the clusters with X-ray counter -parts, **X-ray flux** for all the *Planck* clusters not previously detected in X-ray surveys.

Mollweide projection with the Galactic plane horizontal and the Milky Way centre in the middle, of the
1227 *Planck clusters and candidates across the sky (red thick dots).*
Masked point-sources (black thin dots), Magellanic clouds (large black areas), Galactic mask, covering a total of 16.3% of the sky and used by the SZ-finder algorithms to detect SZ sources.

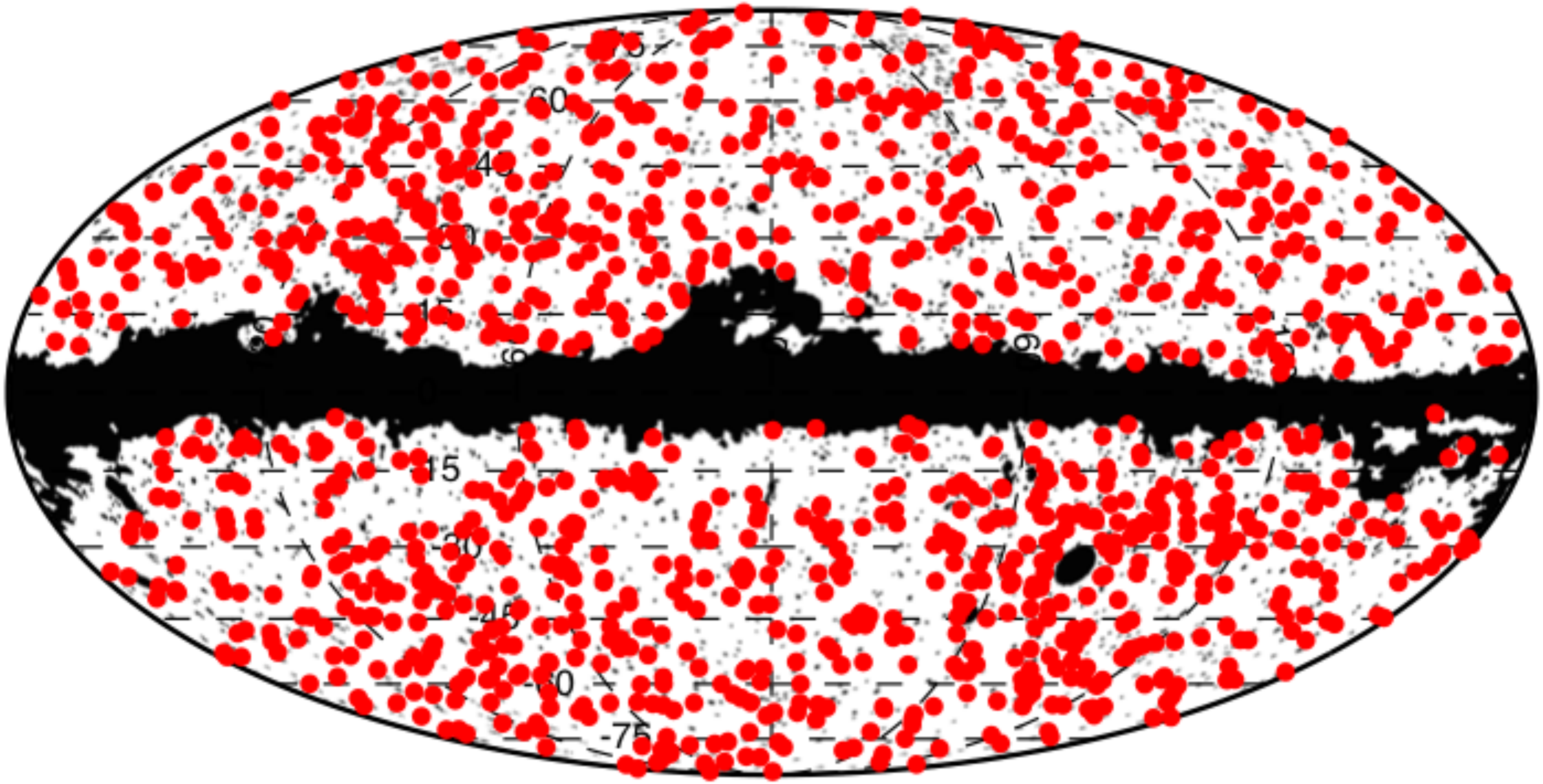

PRISM / COrE+

1

Probing the Universe with galaxy clusters

- The combination of extreme sensitivity, broad spectral coverage, and angular resolution of ***PRISM*** are used to separate the SZ component cleanly from other foregrounds, allowing the following new science:

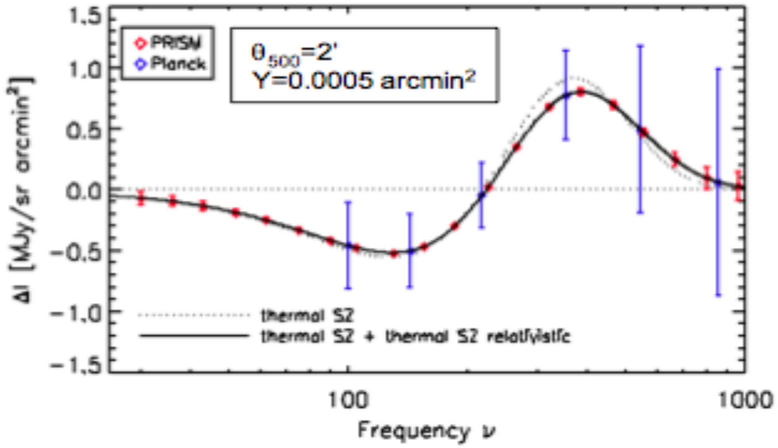

  - detect cluster and groups systems **throughout the Hubble volume** from the moment just after their formation.
  - Measure cluster mass to high redshift (z>4) through gravitational lensing of the CMB (temperature & polarization). **Detection limit below $10^{14}M_{\odot}$ at all redshifts.**
  - Measure the kinetic SZ effect, with typical errors of 50 km/s for individual clusters. **This (and only this) will allow mapping the *cosmic velocity field*. A new probe of dark energy and large scale structure.**

1

Probing the Universe with galaxy clusters

- **Cluster catalog:** realistic simulations show that the PRISM cluster catalogue wil include >10^6 clusters, with mass limit <$10^{14} M_\odot$ at all z.
- **Cosmology probe:** This will allow to constrain cosmological parameters (mainly σ_8 and Ω_m , but also w_a and w_o).
- **Cosmic velocity field**: The peculiar velocity of a few ~10^5 galaxy clusters will be measured
- **Relativistic corrections and non-thermal effects**: the temperature of the hot gas will be measured for ~10^4 galaxy clusters

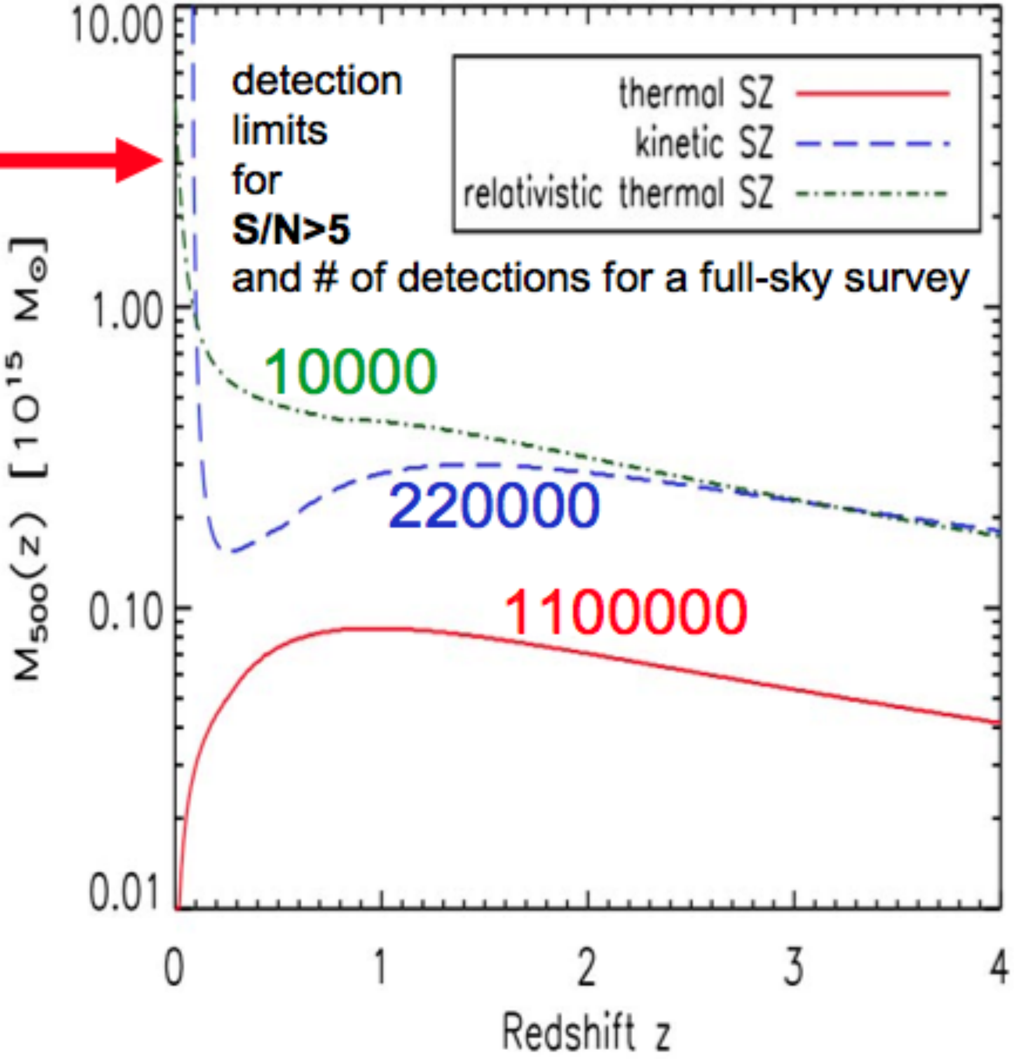

SZ effect with SKA towards galaxy clusters

- The identification of about one thousand of galaxy clusters with the XMM-Newton and *Planck* ESA satellites is on-going, while observations of many thousands of clusters (~ 5×10^5) come from the SDSS.
- The typical angular sizes of galaxy clusters range from ~ arcmin to few tens of arcmin.
- With the the SKA collecting area it will be possible to accurately map the SZ effect of each considered cluster, particularly at moderately high z, with a precise subtraction of discrete radio sources.
- The combination with X-ray images, in particular with those proposed to ESA for the *Athena* satellite project, designed to reach ~ arcsec resolution on a few arcmin FOV, will allow to accurately map the thermal and density structure of the gas in galaxy clusters.
- Also, remarkable will be the synergy with the optical and infrared (IR) surveys at ~ arcsec resolution expected in about ten years from the ESA *Euclid* satellite.

Thermal SZ effect at galaxy scale

- The proto-galactic gas is expected to have a large thermal energy content, leading to a detectable SZ signal, both when the protogalaxy collapses with the gas shock-heated to the virial temperature (Rees & Ostriker '77, White & Rees '78 [3,4]), and in a later phase as the result of strong feedback from a flaring active nucleus (Ikeuchi '81, Platania et al. '02 [5-7]).
- The angular scales of these SZ signals from galaxies are of the order of ≈ 10″, then of particular interest for a detailed mapping with the SKA and *Athena* in the radio and X-ray, respectively.
- The probability of observing these SZ sources on a given sky field at a certain flux detection level and the corresponding fluctuations are mainly determined by the redshift dependent source number density per unit interval of the SZ (decrement) flux.
- The lifetime of the considered SZ sources is crucial to determine their number density.

Thermal SZ effect at galaxy scale

- In general, a direct probe of these models and, possibly, their accurate knowledge through a precise high resolution imaging is highly interesting. The figure in next page shows the number counts at 20 GHz predicted by these models: in a single SKA FOV about few $\times$ 10^2 – 10^3 SZ sources with fluxes above ~ 100 nJy could be then observed in few hours of integration.

- Given the typical source sizes, we expect a blend of sources in the SKA FOV at these sensitivity levels, while much shorter integration times, ~ sec, on many FOV would allow to obtain much larger maps with a significant smaller number of resolved SZ sources per FOV.

- Both surveys on relatively wide sky areas and deep exposures on limited numbers of FOV are interesting and easily obtainable with SKA.

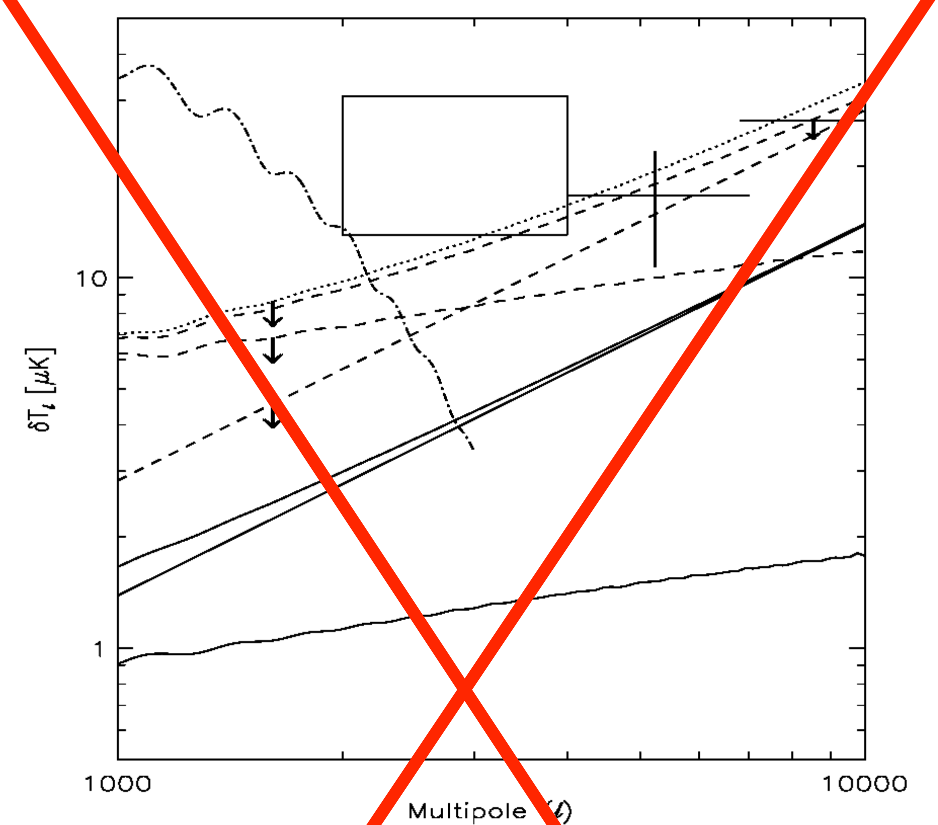

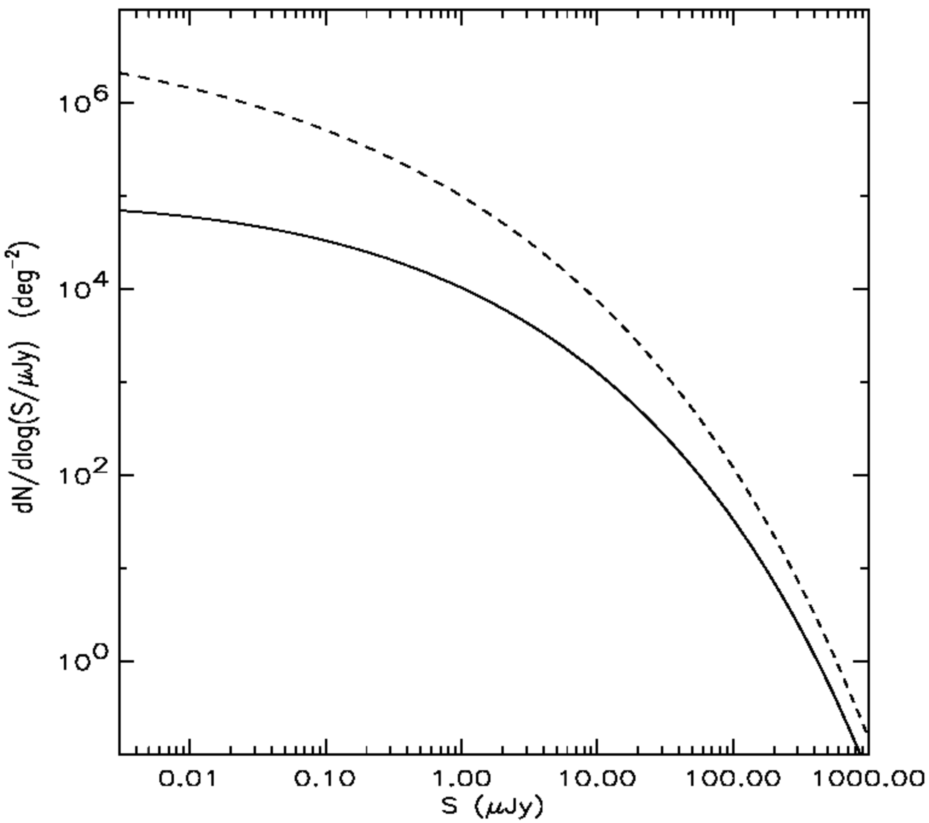

Angular power spectrum of SZ effects at 30 GHz compared to CMB primary fluctuation power spectrum and CBI (box) and BIMA (data points) measures. Solid lines represent clustering (bottom line), Poisson (middle line) and global (upper line) contributions from quasar driven blastwaves. Dashed lines represent clustering (bottom line at high ℓ), Poisson (middle line at high ℓ) and global (upper line) contributions from proto-galactic gas. The latter are actually upper limits since, because of the uncertainty in the cooling time, the extreme assumption that $t_{cool} = t_{exp}$ has been adopted in the computation. Dots refer to the overall contribution. From Burigana et al. '04 [8].

Number count predictions at 20 GHz for SZ effects as function of the absolute value of the flux from proto-galactic gas heated at the virial temperature (dashes) assuming $M_{gas}/M_{vir} = 0.1$ and from quasar driven blast-waves (solid line). The exponential model for the evolving luminosity function of quasars is derived by Pei '95 [9] for an optical spectral index of quasars $\alpha = 0.5$ ($S_\nu \propto \nu^\alpha$). The parameters have been set at $\varepsilon_{BH} = 0.1$, $f_h = 0.1$, $k_{bol} = 10$, $t_{q,opt} = 10^7$ yr. From Burigana et al. '04 [8].

Free-free signals: Ionized halos at high z

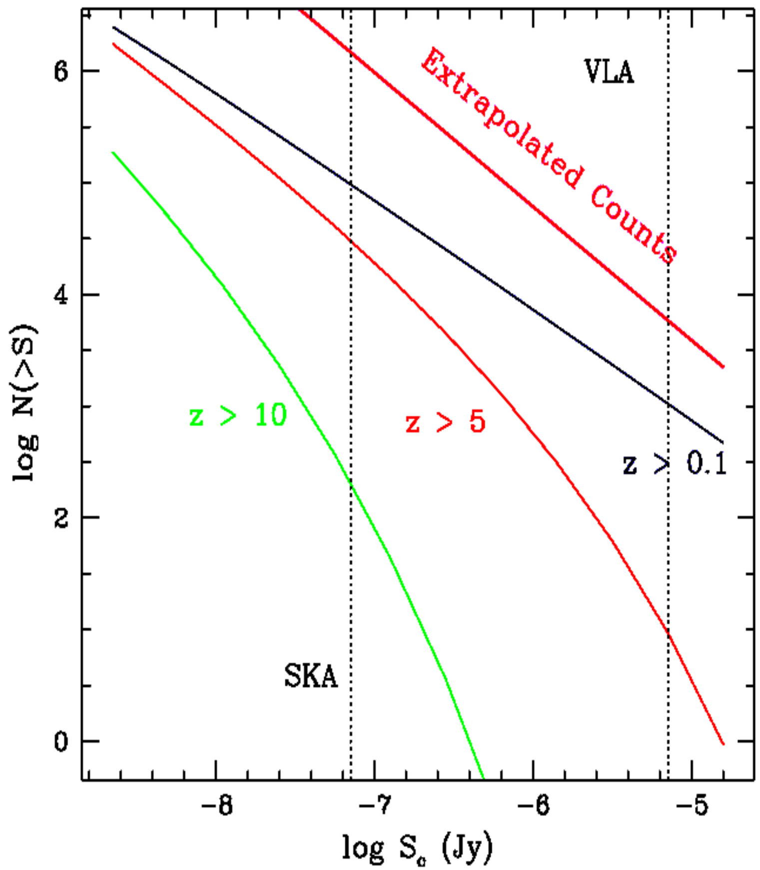

The understanding of the ionizing emissivity of collapsed objects and the degree of gas clumping is crucial for reionization models. The observation of diffuse gas and Population III objects in thermal bremsstrahlung has been investigated by Oh '99 [10]. A natural way to distinguish between free-free distortion by ionized halos is represented by high resolution observations of dedicated sky areas and by the fluctuations in the free-free background.

✧ In this model halos collapse and form a starburst lasting to = 10^7 yr, then recombine and no longer contribute to the free-free background.

✧ By adopting a Press-Schechter model, [] computed the number density of collapsed halos per mass interval and translated it in the cumulative number counts at different fluxes (see figure).

✧ SKA will allow to detect bright sources with deep exposures. SKA should be able to detect ~ 10^4 individual free-free emission sources with z > 5 in 1 □ above a source detection threshold of 70 nJy.

Number of sources which may be detected in the 1□ by SKA, as a function of the threshold flux S_C. Realistic limiting fluxes for point source detection are shown. The extrapolated source counts from Partridge et al. '97 [11] are also shown. From Oh '99 [10].

Free-free signals:
Individual halo at moderate z

Massive and dense clusters would produce a strong signal making the study of free-free emission in clusters at radio frequencies an interesting and useful way to study the intracluster medium.

✧ The figure shows a map of the free-free signal at 1 GHz extracted from a 300 Mpc simulation. The free-free distortion is of the order of 1 mK in the cluster regions.

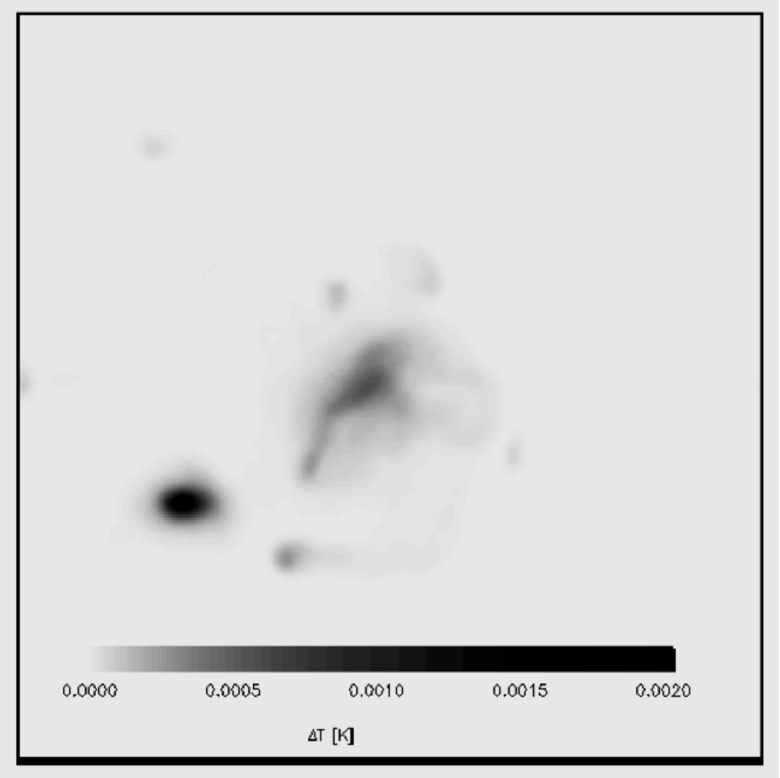

Free-free distortion for a massive halo,
$M = 6.6 \times 10^{14} h^{-1} M_\odot$, at redshift $z = 0.15$.
The greyscale shows the distortion in K and at 1 GHz.
The field of view is ≈ 40′.
The total flux in this region is
$S_{ff} = 2.83 \times 10^{-5}$ Jy.
From Ponente et al. '11 [12].

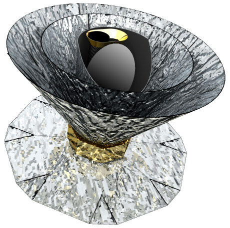

CMB spectral distortions

❖ Current observations *consistent with Blackbody & Standard Big-Bang Model* **… but:**

- **Very small distortions** in continuum spectrum are
  - ❖ **strongly predicted** to be generated during ***late epochs*** (z < 10^4), as Comptonization, free-free distortions associated to **reionization / structure formation**, hot galaxy clusters: **clearly detectable by PRISM (≳100σ!)**
  - ❖ **or may be produced or have to be produced** at ***earlier epochs***
    (Bose-Einstein distortions, intermediate shapes, "exotic shapes") by "exotic" processes, as decays, annihilation, cooling/Bose condensation, damping of primordial perturbations probing the *power spectrum on very small scales (inflation)*: **detectable by PRISM → New physics!**
- **→ "Direct" reconstruction** of thermal history & thermodyn. processes **up to z ≅10^7**
- ➢ N.B.: fully analogy with CMB anisotropy before COBE/DMR:
  Standard model would be untenable if no distortion were detected

➢ **H & He recombination lines from z ≃ 10^3**

➢ *HI Balmer & Paschen-α lines detectable with* ***PRISM***

➢ ***additional anisotropic signal detectable with PRISM***

➢ **Resonant scattering signals of metals during the *dark ages***

Astrophysical models:
CMB Comptonization distortions from reionization

	Suppression	Filtering
u	1.69×10^{-7}	9.65×10^{-8}
$u(z \geq 6)$	7.98×10^{-8}	1.05×10^{-8}

(C.B. et al. 2008, MNRAS, 385, 404)

Compatible with FIRAS limits → call for next generation CMB experiments (FIRAS II, DIMES, Moon Based ideas,

PIXIE – Kogut et al. 2011, JCAP, 7, 25, PRISM Coll. 2013, 2014)

Free-free distortions: effect of clumping

- **The homogeneous approximation is a rough lower limit approximation for free-free, because of the $(\Omega_b)^2$ dependence implying an amplification factor, related to P(k) (and DM particle properties)**

$$\frac{\langle \rho^2 \rangle}{\langle \rho \rangle^2} = 1 + \frac{\langle (\delta\rho)^2 \rangle}{\langle \rho \rangle^2} = 1 + \sigma^2 > 1$$

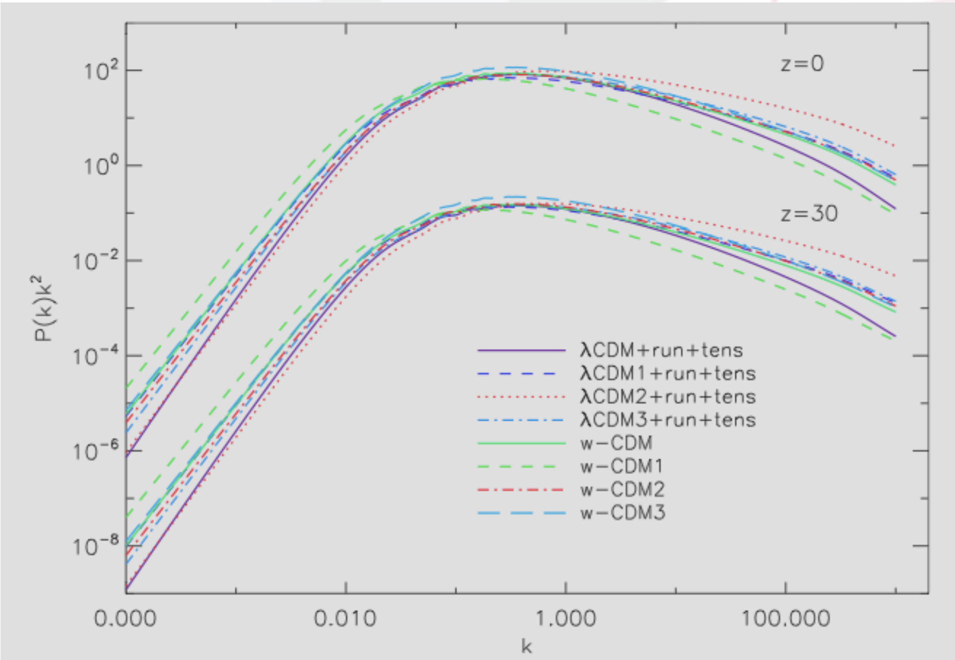

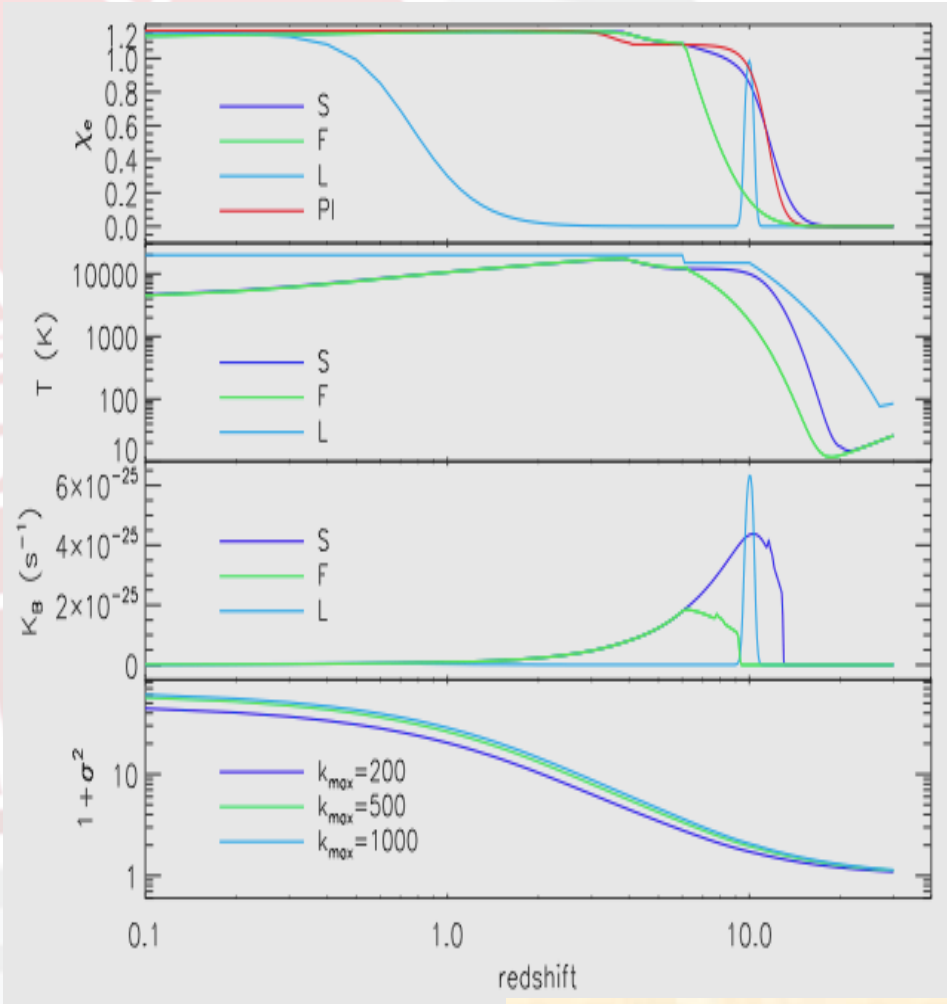

T. Trombetti & C.B. 2014, MNRAS 437, 2507

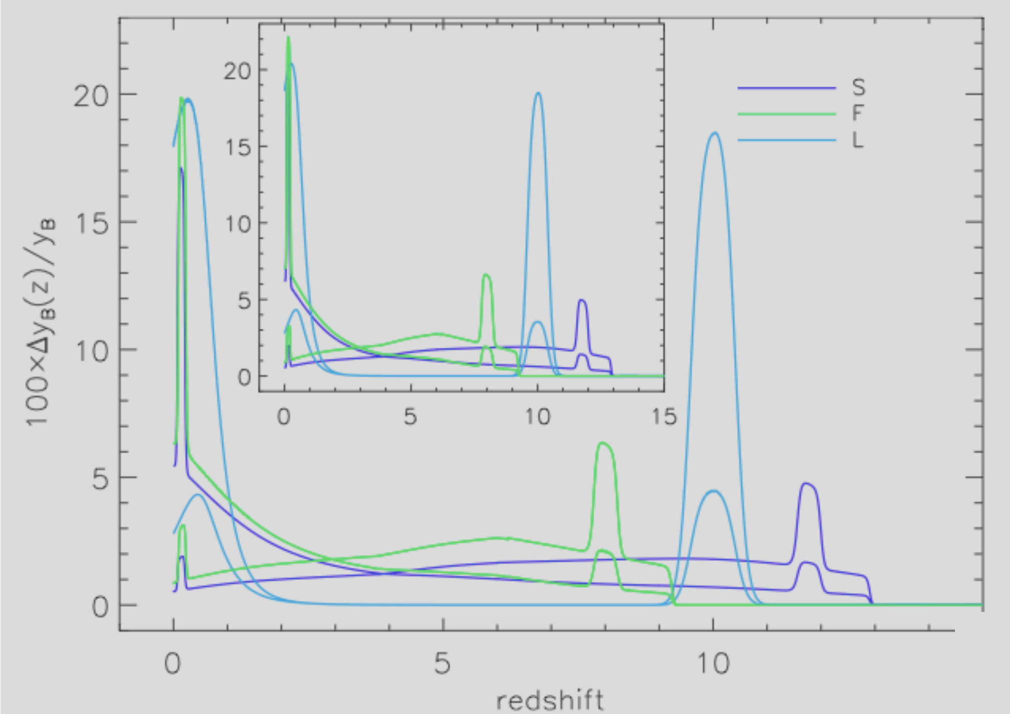

Relative contribution peaks when the process starts and at low z

✓**Spectral shape sligthy steeper than λ^2 (because of Gaunt factor)**
✓**Note the amplification by clumping, increasing for increasing k_{max}**
✓**(Negative) FF by cooling largely subdominant**

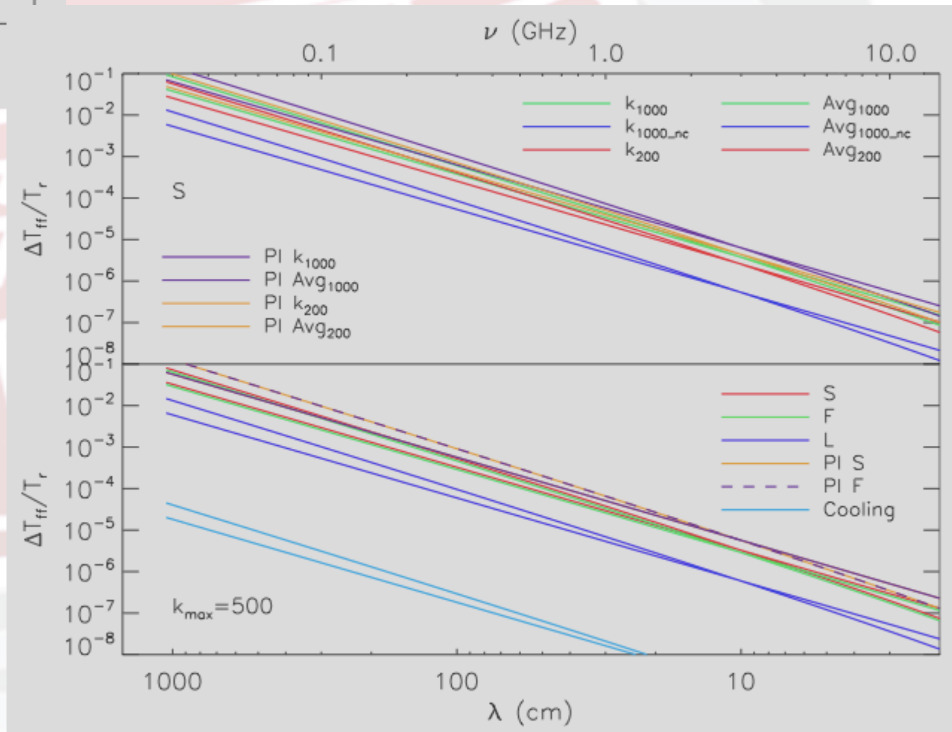

❖Without any particular assumption about complex haloes physics, **the global averaged free-free distortion signal expected from the diffuse ionized IGM** in a given cosmological reionization scenario can be derived from fundamental arguments based only on **density contrast evolution** on cosmological models and well-known radiative emission mechanisms

(T. Trombetti & C.B. 2014, MNRAS 437, 2507):

- ✓ Boltzmann codes for the matter variance evaluation;
- ✓ a dedicated code for the free-free distortion including the correct time and frequency dependence of Gaunt factor.

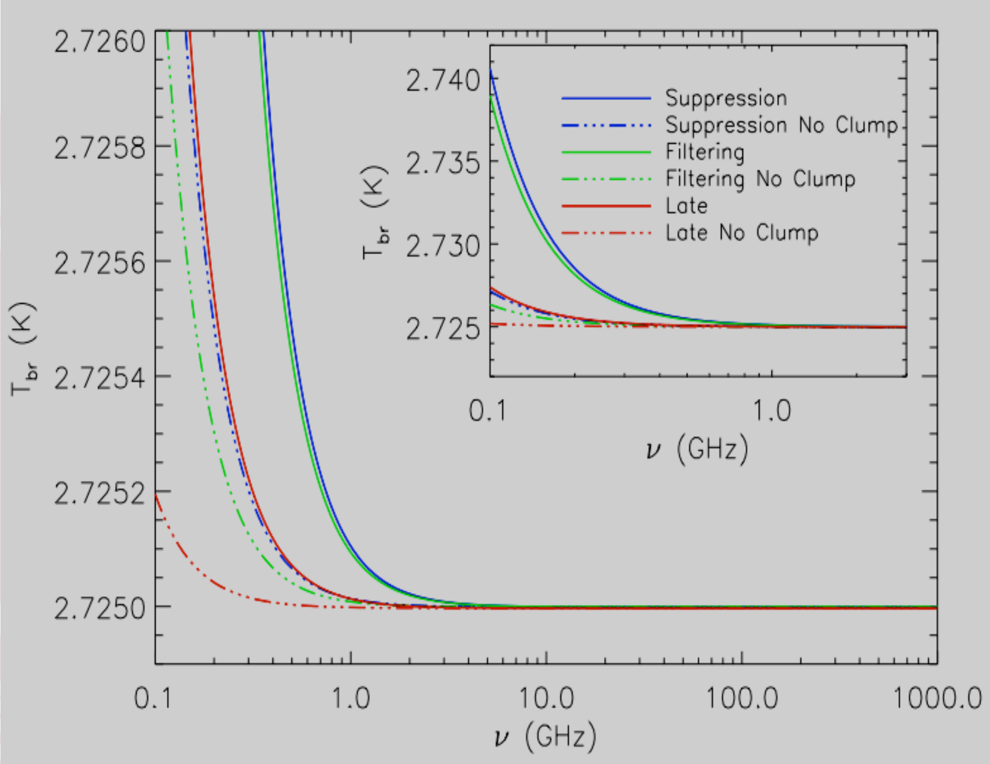

The expected excess is at ~ mK level at decimeter wavelengths **a target clearly accessible to the SKA sensitivity. To firmly detect this signal it is necessary to accurately observe the diffuse background level.** FF signal is a few % of Comptonization decrement expected in these models at $\lambda < 1$ cm (here signals from both free-free distortion and Comptonization decrement are included).

✧Ponente et al. ‘11 [12] studied the regime of more massive halos focusing on the post reionization era, studying free-free radio emission from ionized gas in clusters and groups of galaxies with analytical models and simulations.

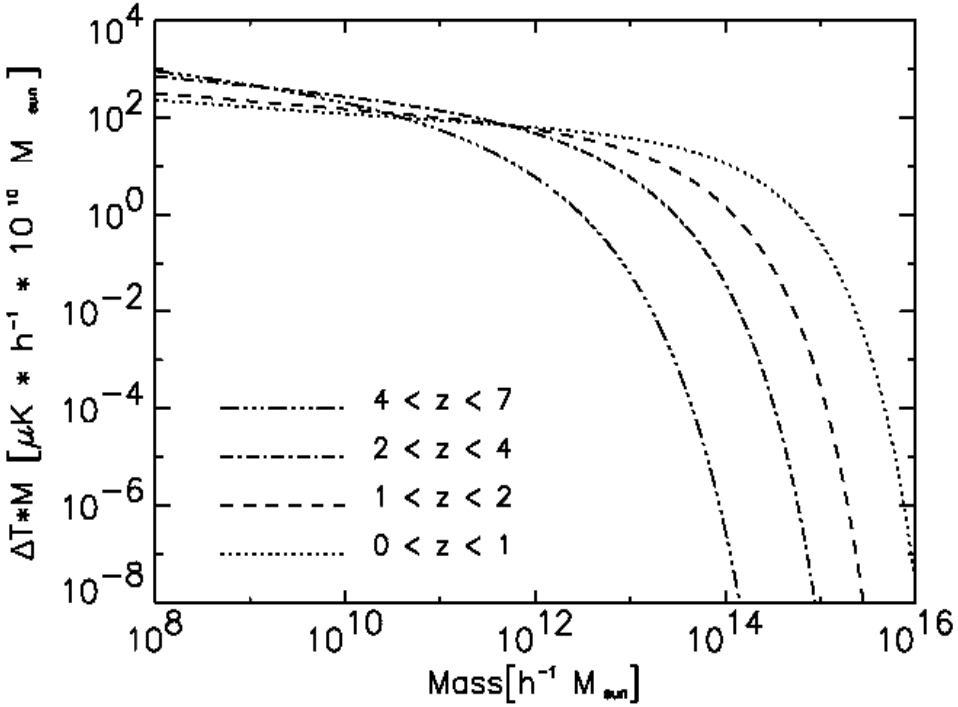

The figure shows the dependency of the average free-free distortion with the mass range for different redshift intervals. Smaller haloes contribute more to the average signal than massive ones at all redshifts. From Ponente et al. ‘11 [12].

✧ The cooling time is notably larger for massive haloes and highly non-linear phenomena like radiative cooling can be more easily ignored.

✧ **Combining a halo gas distribution model, as the β-model, with the haloes abundance as function of mass and redshift, it is possible to compute the mean free-free signal in a solid angle, function of redshift and/or mass.**

SKA contribution to future CMB spectrum experiments

- The current limits on CMB spectral distortions and energy dissipation processes in the plasma, $|\Delta\varepsilon/\varepsilon_i| \leq 10^{-4}$, are mainly set by the NASA COBE/FIRAS experiment.
- High accuracy CMB spectrum experiments from space, like DIMES at $\lambda \geq 1$ cm and FIRAS II at $\lambda \leq 1$ cm, have been proposed to constrain (or probably detect) energy exchanges 10–100 times smaller than the FIRAS upper limits possibly generated by heating (but also by cooling) mechanisms at different cosmic epochs.
- These perspectives have been recently renewed in the context of a new CMB space mission like PIXIE proposed to NASA or even in the possible inclusion of spectrum measures in the context of a polarization dedicated CMB space mission, of high sensitivity and up to arcmin resolution, like PRISM proposed to ESA.

To firmly observe such small distortions the Galactic and extragalactic foreground contribution should be accurately modelled and subtracted.

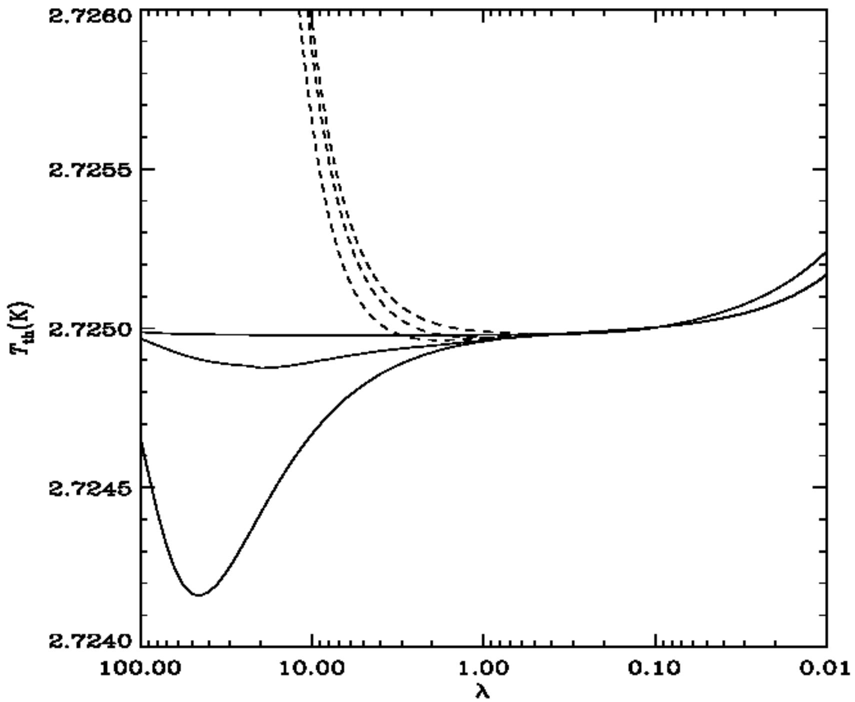

CMB distorted spectra as functions of the wavelength λ (in cm) in the presence of a late energy injection with $\Delta\varepsilon/\varepsilon_i \simeq 4y = 5 \times 10^{-6}$ plus an early/intermediate energy injection with $\Delta\varepsilon/\varepsilon_i = 5 \times 10^{-6}$ occurring at the "time" Comptonization parameter $y_h = 5, 1, 0.01$ (from the bottom to the top; in the figure the cases at $y_h = 5$ – when the relaxation to a Bose-Einstein modified spectrum with a dimensionless chemical potential given, in the limit of small distortions, by $\mu \simeq 1.4\Delta\varepsilon/\varepsilon_i$ is achieved – and at $y_h = 1$ are extremely similar at short wavelengths; solid lines) and plus a free-free distortion with $y_B = 10^{-6}$ (dashes). From Burigana et al. '04 [8].

- The very faint tail of radio source counts is essentially unexplored and their contribution to the radio background at very low brightness temperature is not accurately known.
- For illustration, with reasonable assumptions on differential source number counts, we find a contribution to the radio background at 5 GHz from sources between ~ 1 nJy and ~ 1 μJy between few tens of μK and few mK.
- These signals are clearly negligible compared to the accuracy of current CMB spectrum experiments, in particular at $\lambda > 1$ cm, but are significant at the accuracy level on CMB distortion parameters potentially achievable with future experiments.
- Differently from Galactic emission, it is isotropic at the angular scales of few degrees and can not be then subtracted from the CMB monopole temperature on the basis of its angular correlation properties.
- A direct radio background estimate from precise number counts will certainly improve the robustness of this kind of analyses.

- The relevance of this problem emerged in the detection by the NASA ARCADE 2 of an excess in the CMB absolute temperature at 3.3 GHz. Although this excess and its interpretations are controversial, this underlines how crucial is the precise estimation of very faint source counts for the exploitation of precise CMB spectrum measures.
- The SKA sensitivity at 20 GHz will allow the detection (to 5σ) of sources down to a flux level of ≃ 200 nJy (≃ 60,20,6 nJy) in 1 (10, 10^2, 10^3) hour(s) of integration over the ≃ 1 mas (FWHM) resolution element; similar numbers (from ≃ 250 to 8 nJy in an integration time from 1 to 10^3 hours, respectively) but on a resolution element about 10 times larger will be reached at ≈ GHz frequencies by using a frequency bandwidth of about 25%.
- Therefore, the SKA accurate determination of source number counts down to very faint fluxes can directly help the solution of one fundamental problem of the future generation of CMB spectrum space experiments at $\lambda > 1$ cm.

Summary of CMB spectral distortions in intensity

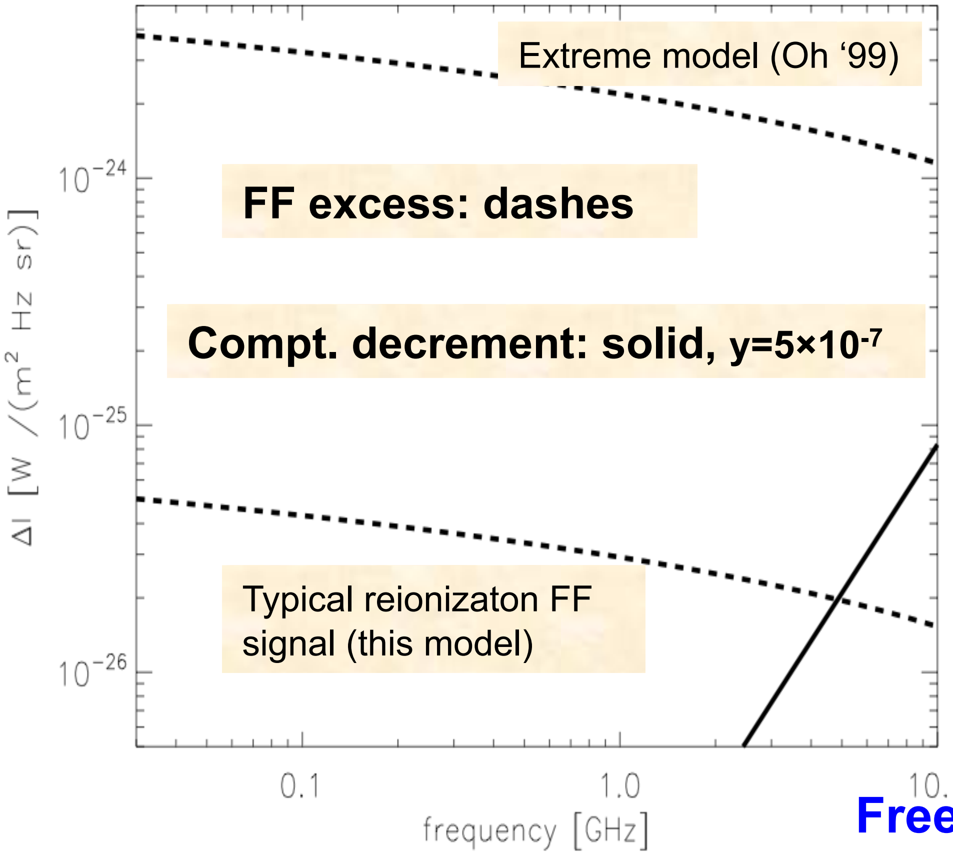

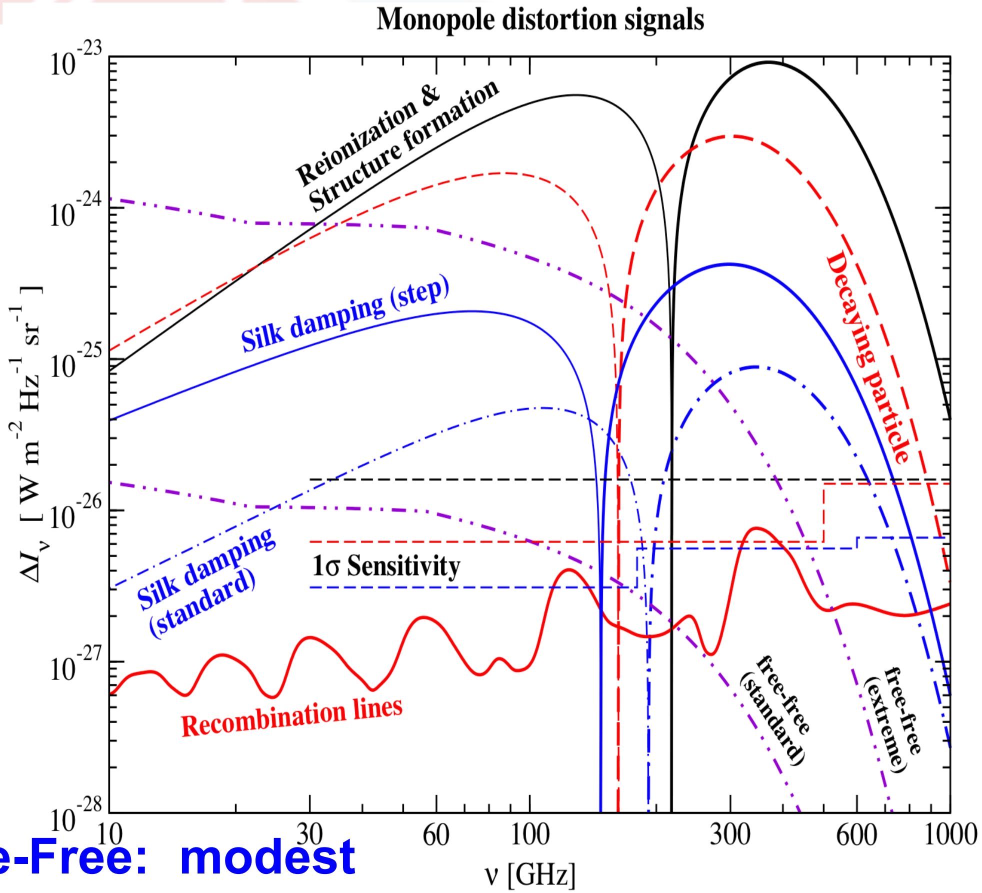

Free-Free: modest but not negligible impact for CMB space missions, main target for ground-based observations.

Low freqs.

Ground experiments, DIMES, ARCADE 2, SKA & its precursors

High freqs.

FIRAS II, Pixie, PRISM

From PRISM studies

Cross-correlations between (radio source) catalogs & CMB maps

✧ High accuracy CMB surveys, like *Planck*, typically cover a high sky fraction, f_{sky}, or even the whole sky. The SKA is mainly designed to achieve very faint fluxes on limited sky fields.

✧On the other hand, the sensitivity of the SKA (SKA2_mid_dish in particular, but also SKA precursors) is so high on typical FoVs of ~ degree side at frequencies around one GHz, that it is reasonable to think to cover a significant sky fraction (thousands of square degrees) with unprecedented sensitivity accumulating some months of integration.

✧ A 1-yr SKA survey will contain > $10^9(f_{sky}/0.5)$ HI galaxies in at redshifts $0 < z < 1.5$.

✧ This makes the combination of *Planck* and SKA a powerful tool for improved cross-correlation analyses between CMB and radio data, that can be generalized to surveys in other frequency bands.

Cross-correlations between radio source catalogs & CMB maps

Cross-correlation & angular power spectrum

Given a CMB map in temperature and a galaxy survey x = (T, G) (vector in pixel space), the Quadratic Maximum Likelihood (QML) (Tegmark '97 [15]) provides an estimator of the angular power spectrum C_ℓ^X, with X being one of TT, TG, GG.

The QML estimator is well suited for such analysis for several reasons:

- ✓ **it is optimal (i.e. unbiased and minimum variance);**
- ✓ **it is a computationally demanding method and can be currently applied only at modest resolution but this is not a problem for studying effects present at large angular scales for which where the computation is affordable on a supercomputer;**
- ✓ **it is pixel based, making trivial the masking process necessary because of foreground emission or incomplete sky coverage.**

Applications to ISW effect – I

✧ The Integrated Sachs Wolf (ISW) effect results from the line of sight integral in the Sachs-Wolfe ‘67 equation [16]. It arises when CMB photons streaming across the Universe interact with the time evolving gravitational potential wells associated with the foreground large scale structure.

✧ The potential evolution leads to a net change of the photon energies as they pass through them. The ISW is a linear effect depending on the cosmological model, since it requires a change in equation of state of the cosmic fluid.

✧The evolution/variation of the gravitational potential is related to the linear density perturbations of matter. This change is important at early times, when the universe goes from being radiation dominated to matter dominated (early ISW), and at late times, as the dark energy (or curvature) takes over from the matter (late ISW).

✧ Unlike the early ISW, the late ISW is virtually uncorrelated with the CMB anisotropies generated at last scattering: the typical auto-correlation function for the ISW is shown in figure (from Crittenden et al ’96 [17]) of next slide for a ΛCDM model.

Applications to ISW effect – II

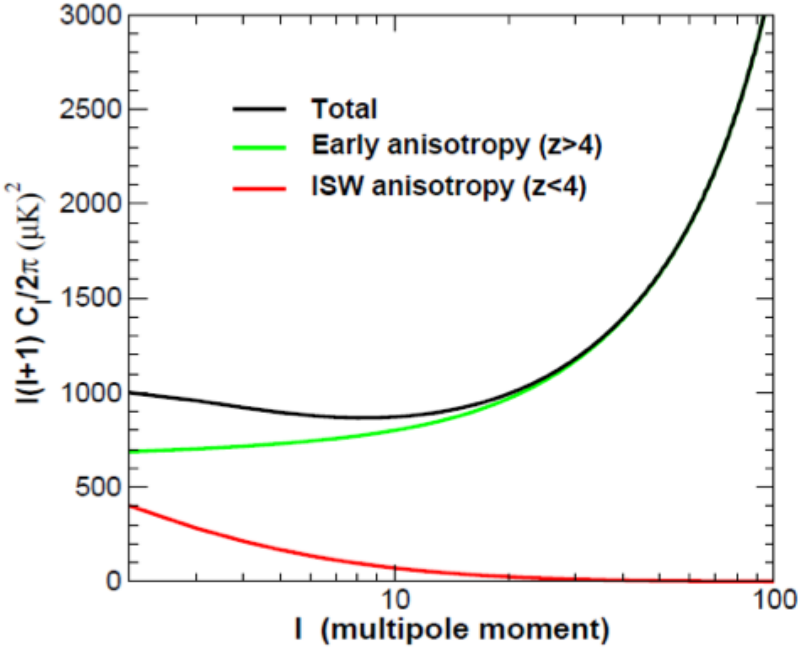

➢ **It is advantageous to isolate the late ISW generated at low redshifts through the cross-correlation of the CMB maps with LSS surveys:**

✓ CMB photons cross a time-varying potential and become slightly hotter or colder

➢statistically, we expect a tiny correlation of hot spots in the CMB with LSS, an effect which expected to be less than 1 μK.

➢ **Interesting results have been already achieved from cross-correlating WMAP & SDSS and WMAP & NVSS (Raccanelli et al. '08, Schiavon et al. '12 [18,19]), opening the road for *Planck* & SKA analyses.**

Non-Gaussianity … mainly through CMB bispectrum

$$B^{m_1 m_2 m_3}_{\ell_1 \ell_2 \ell_3} \equiv \langle a_{\ell_1 m_1} a_{\ell_2 m_2} a_{\ell_3 m_3} \rangle$$

$$= \mathcal{G}^{\ell_1 \ell_2 \ell_3}_{m_1 m_2 m_3}\, b_{\ell_1 \ell_2 \ell_3}$$

Gaunt integrals

$$\mathcal{G}^{\ell_1 \ell_2 \ell_3}_{m_1 m_2 m_3} \equiv \int Y_{\ell_1 m_1}(\hat{\boldsymbol{n}})\, Y_{\ell_2 m_2}(\hat{\boldsymbol{n}})\, Y_{\ell_3 m_3}(\hat{\boldsymbol{n}})\, d^2\hat{\boldsymbol{n}} = h_{\ell_1 \ell_2 \ell_3} \begin{pmatrix} \ell_1 & \ell_2 & \ell_3 \\ m_1 & m_2 & m_3 \end{pmatrix},$$

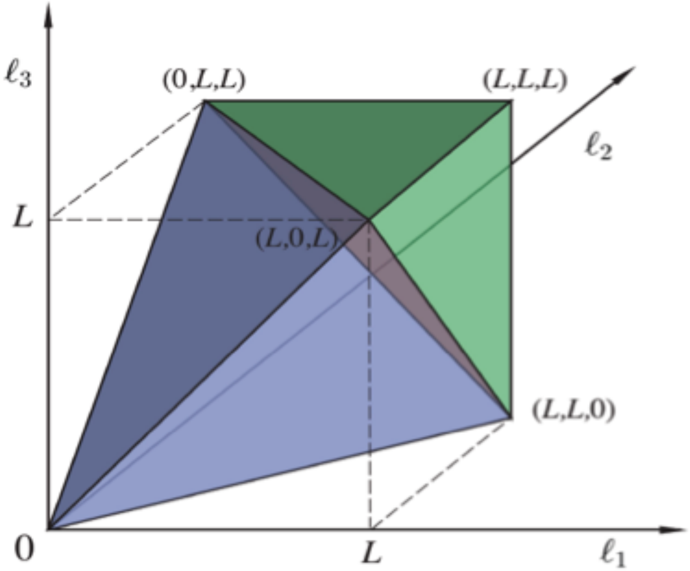

Triangle condition: $\ell_1 \leq \ell_2 + \ell_3$ for $\ell_1 \geq \ell_2, \ell_3$, +perms.

Parity condition: $\ell_1 + \ell_2 + \ell_3 = 2n\,, \quad n \in \mathbb{N}\,,$

Resolution: $\ell_1, \ell_2, \ell_3 \leq \ell_{\max}\,, \quad \ell_1, \ell_2, \ell_3 \in \mathbb{N}\,.$

(1) Multiple fields (local models, non-linearities develop outside horizon)

(2) Non-canonical kinetic term of quantum fields (higher derivative interactions; Dirac-Born-Infeld, K-inflation)

(3) Non-vacuum initial conditions

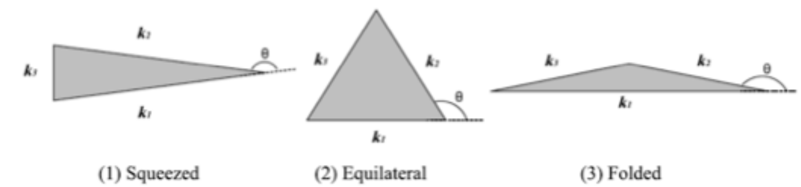

+ many more

f_{NL} from *Planck* data

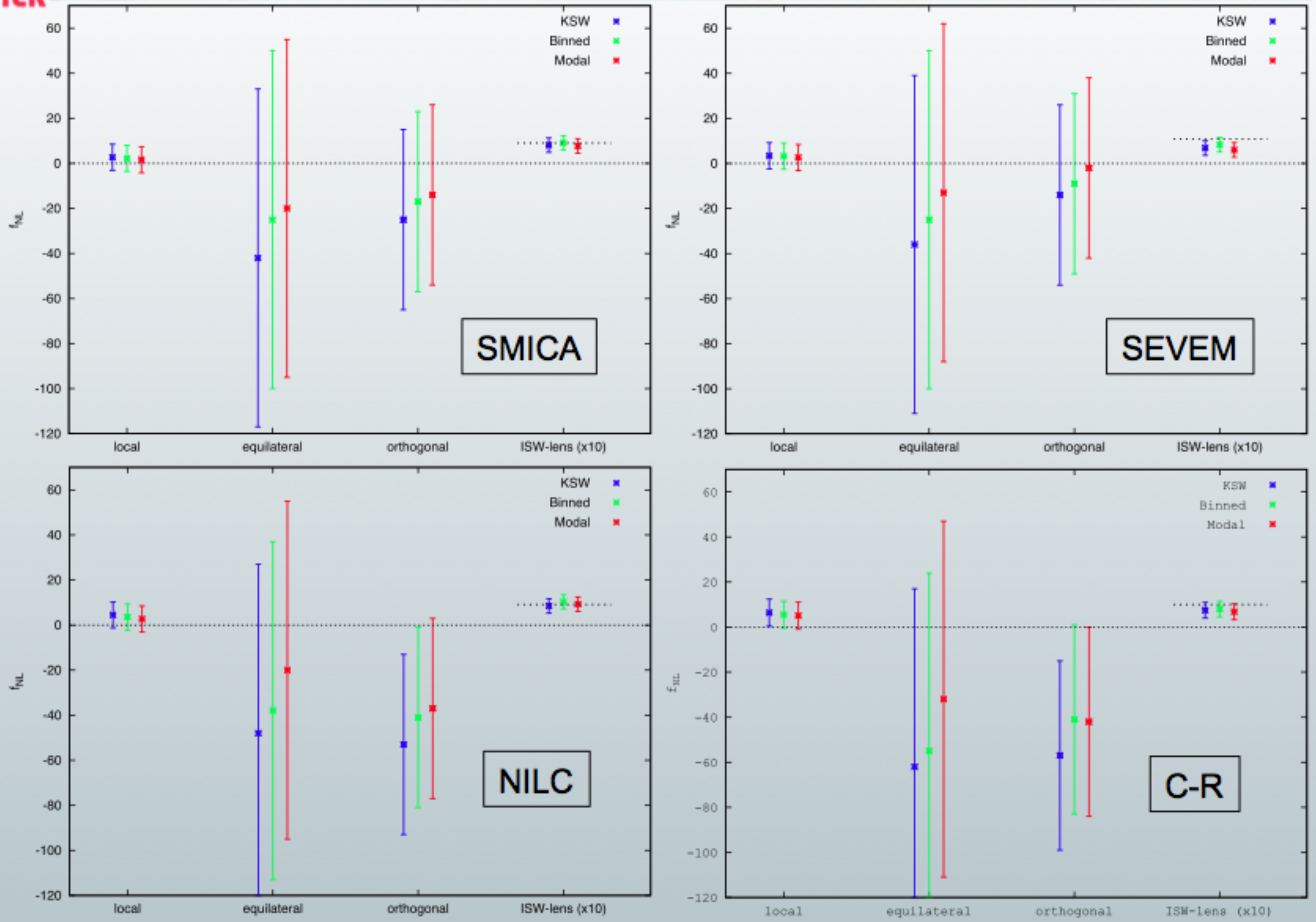

C. Burigana, Paris, Chalonge 2014

CMB & (radio)galaxy surveys → non-Gaussianities

- Primordial perturbations at the origin of the LSS may leave their imprint in the form of small deviations from a Gaussian distribution. Different kinds of configurations, such as the so-called local type, equilateral, enfolded, orthogonal, have been predicted. Their detection would have profound implications for inflationary mechanisms.
- Extragalactic radio sources are particularly interesting as tracers of the LSS, since they span large volumes up to high redshifts. **Radio sources from NVSS**, quasars from SDSS DR6 and DR7, LRG from SDSS II have been recently analyzed by Xia et al. '11 [20] also in combination with **WMAP map**:
  - **f_{NL} = 48±20, 50±265, 183±95 at 68% CL for local, equilateral, enfolded configurations**

- **Huge progress expected combining Planck & SKA (& Euclid)**

SKA sensitivity to APS

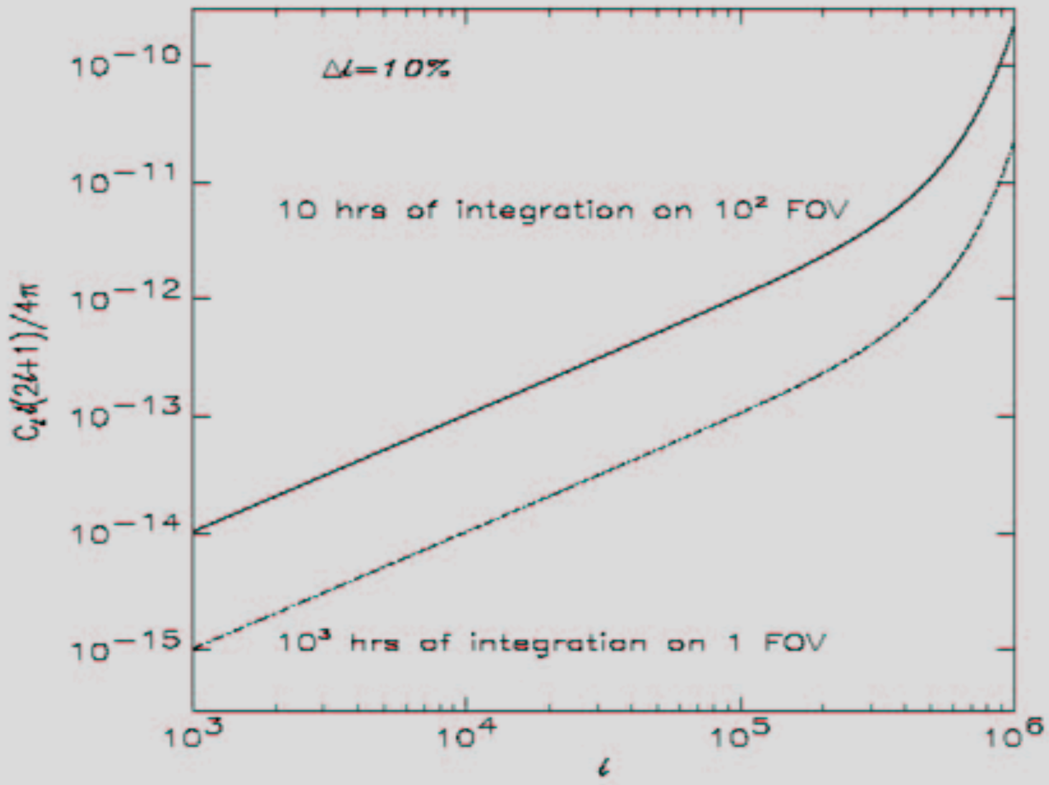

Absolute uncertainty on dimensionless CMB angular power spectrum recovery due to the instrumental noise for some reference cases.

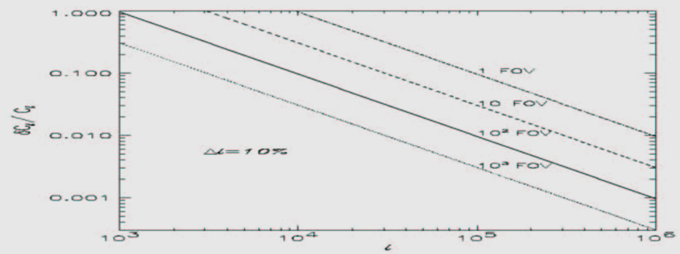

Relative uncertainty on CMB angular power spectrum recovery from combined cosmic and sampling variance for some representative sky coverages. As evident the sky coverage corresponding to $\sim 10^2$ SKA FOV (or to ~ 1 SKA FOV) allows to reach a relative "fundamental" uncertainty less than $\simeq 10\%$ at $\ell \simeq 10^4$ (or at $\simeq 10^5$) and significantly smaller at larger multipoles.

Primordial magnetic fields (PMF)

✧ Large scale magnetic fields of the order of few μG observed in galaxies and galaxy clusters may be the product of the amplification, during structure formation, of primordial magnetic seeds (Ryu et al. ‘12 [21]).

✧ Models of early Universe predict the generation of PMF, either during inflation or during cosmological phase transitions (Widrow et al. ’12 [22]).

✧ Constraints at the nG level come from CMB temperature power spectrum and bispectrum (Paoletti & Finelli ‘11, Caprini et al. ‘09 [23,24]).

✧ Gamma ray observatory *Fermi* have added new intriguing observations which might be interpreted as a lower bound for the amplitude of PMF.

✧ The data on gamma ray cascades from Blazars show a lack of photons which is compatible with diffuse extra-galactic magnetic fields in the intracluster medium (voids) with a lower bounds of the order of $10^{-15} - 10^{-16}$ G (Neronov & Vovk ‘10 [25]).

Primordial magnetic fields (PMF)

✧ If this lower bound for PMF will be confirmed, SKA can perform crucial measurements towards the probe of the generation mechanism.

✧ SKA measurement of very high-ℓ multipoles can improve these bounds on PMF as well as the characterization of foreground and secondary anisotropies beyond the Silk damping tail.

✧ The smoking gun of the Faraday rotation of CMB polarization anisotropies from intervening magnetic fields from a stochastic background of PMF is a B-polarization signal at very high-ℓ multipoles, $\ell \sim 10^4$.

✧ SKA observations can target such signal.

Galactic foregrounds versus Galactic astronomy

The accurate study of Galactic emissions is crucial for any cosmological exploitation of radio to infrared sky. In this context, Galactic emissions are considered as sources of foreground.

- As first probed by DASI, interferometers can be fruitfully used to map the diffuse sky signal on relatively wide areas in both total intensity and polarization, Fourier transforming data from the U-V space to the real 2D space.
- The possibility of extending this opportunity to intermediate and large scales, or equivalently to low and intermediate multipoles, largely relies on the capability of available mosaic techniques to assemble different FoVs into maps with appropriate large scale calibration and matching. This is of increasing complexity at SKA increasing frequency, since the smaller FoV sizes of higher frequencies. **Also, recalibration of SKA FoVs with precursors (ASKAP-PAF, Meerkat) maps could be in principle exploited.**
- On the other hand, the high Galactic radio signal does not require the extreme accuracy demanded, for instance, by CMB fluctuation mapping at the SKA highest frequencies.

Galactic foregrounds versus Galactic astronomy

❖ **The SKA radio frequency coverage is of extreme interest to study the Galactic synchrotron emission, in both total intensity and polarization, and the unpolarized Galactic free-free emission.**

❖ **Extending the SKA frequency coverage to highest frequencies will allow to accurately derive the spectral behaviour of these emissions on a wide range. This is crucial for the accuracy of many component separation methods. In fact:**

- ✓ they take great benefit by the increasing of the frequency range of the templates adopted in the analysis and/or by a priori information about the spectral behaviour of the different components, related to the energy and properties of emitting particles, superimposed in the overall signal
- ✓ this information contributes to the improvement of the physical knowledge of the so-called mixing-matrix adopted in the inversion process that derives the different physical components from multifrequency maps.

❖ **Furthermore, SKA data can be used to map the Galactic HI 21-cm emission.**

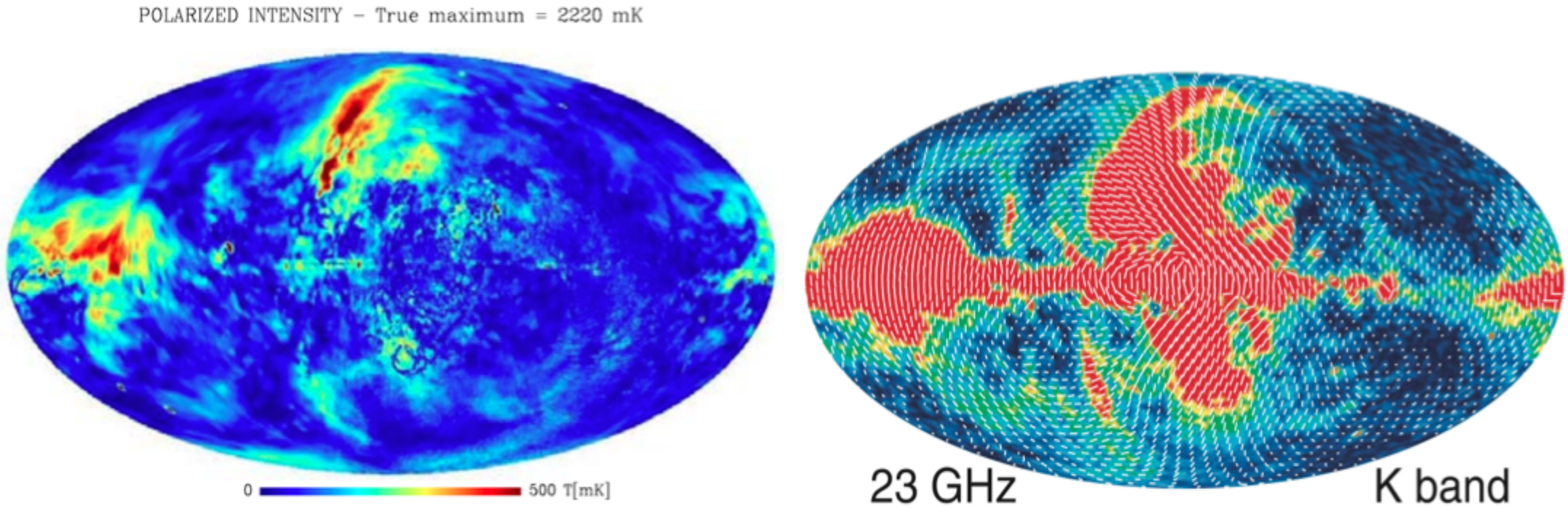

All-sky maps of Galactic polarized emission @ radio (1.4 GHz, left image; from Burigana et al. ‘06 [26]) and @ microwave (23 GHz, right image; from Bennett et al. ‘13 [27]) frequencies.

Regarding the synchrotron emission, produced by relativistic cosmic ray electrons spiralling in the Galactic magnetic field, a remarkable feature of the Galactic radio sky is the significant depolarization appearing in a wide region around the Galactic center.
This effect is certainly much less relevant in the microwaves, as evident by the comparison of available radio surveys with millimeter surveys.

- **If mosaic techniques will work successfully, a view of a very wide sky fraction will allow to map Galactic foregrounds at intermediate and large scales. This will have a tremendous impact for 3D physical models of the Galaxy and for the study of the large scale, almost regular component of the Galactic magnetic field.**
- **Turbulence phenomena predict a typical power law dependence of the power spectrum of diffuse emission with properties related to the physical conditions of the ISM in the considered area.**
- **Almost independently of the accuracy of mosaic techniques, SKA maps on many patches of sky of limited area will allow to reconstruct with unprecedented accuracy the correlation properties of the radio sky diffuse emission, thus providing crucial information for the comparison with theoretical models and and their implementation through numerical codes.**

Multifrequency, high sensitivity radio observations with the SKA will certainly put a firm light on this problem, allowing to disentangle between the various depolarization effects:

- ➢Faraday depolarization associated to Galactic magnetic fields
- ➢geometrical depolarization coming from the averaging in the observed signal of contributions from cells with different polarization angles:
  - ✓along the line of sight
  - ✓within the angular directions of the observational effective beam.

Two other topics crucial for both Galactic science and foreground treatment for cosmology are the understanding of:

✓anomalous microwave emission

✓haze component

SKA will map the low frequency tail of these emissions.

Conclusions

- A next CMB mission is crucial … & desired !
  - ✓ CMB polarization & distortions, recombination lines, clusters, far-IR galaxies/CIB, lensing, Galactic science, etc.
- Forthcoming/future radio facilities are promising!
- LOFAR, SKA & its precursors will answer to fundamental questions … & likely will raise new questions
- Complementarity/synergy between projects/analyses will be fundamental … & the future will be bright !